# Heavy Flavor in medium from lattice QCD

Peter Petreczky

Brookhaven National Laboratory

- Introduction: lattice QCD, spectral functions etc
- NRQCD with extended meson operators and bottomonium properties at $T>0$
- Complex potential at $T>0$
- Thermodynamics of charm
- Heavy quark diffusion coefficient from lattice QCD

# Finite Temperature QCD and its Lattice Formulation

$$\langle O \rangle = \mathrm{Tr} O e^{-\beta H - \mu N}$$

$\beta = 1/T$

evolution operator in imaginary time

$$\langle O \rangle = \int \mathcal{D}A_\mu \mathcal{D}\psi \mathcal{D}\bar{\psi} O e^{-\int_0^\beta d\tau d^3x \mathcal{L}_{QCD}}$$

$$A_\mu(0, \mathbf{x}) = A_\mu(\beta, \mathbf{x}) \quad \psi(0, \mathbf{x}) = -\psi(\beta, \mathbf{x})$$

Integral over functions → (Lattice) → integral with very large (but finite) dimension ( > 1000000 )

$$\langle O \rangle = \int \prod_x dU_\mu(x) O(det M[U, m, \mu]) e^{-\sum_x S_G[U(x)]}, U_\mu(x) = e^{igaA_\mu(x)}$$

$\mu = 0$ → Monte-Carlo Methods

continuum limit $a \to 0$

$N_\tau \to \infty, \ N_\sigma / N_\tau$ fixed

Costs : $\sim m^{-1}$

$\sim a^{-7} \sim N_\tau^7$

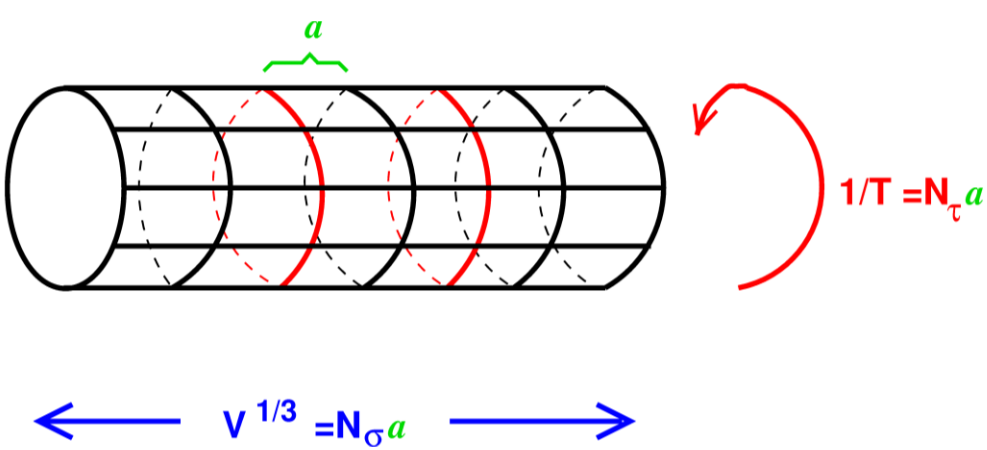

# Meson correlators and spectral functions

Vacuum and in-medium properties as well as dissolution of mesons are encoded in the spectral functions:

$$\rho(\omega,p,T) = \frac{1}{2\pi}\int_0^\infty dt e^{i\omega t}\int d^3x e^{ipx}\langle[O(x,t),O(0,0)]\rangle_T, \quad O(x,t)\sim \bar{Q}(x,t)\Gamma Q(x,t)$$

Melting is seen as progressive broadening and disappearance of the bound state peaks

Modifications of quarkonium yields in heavy ion collisions Matsui and Satz, PLB 178 (1986) 416

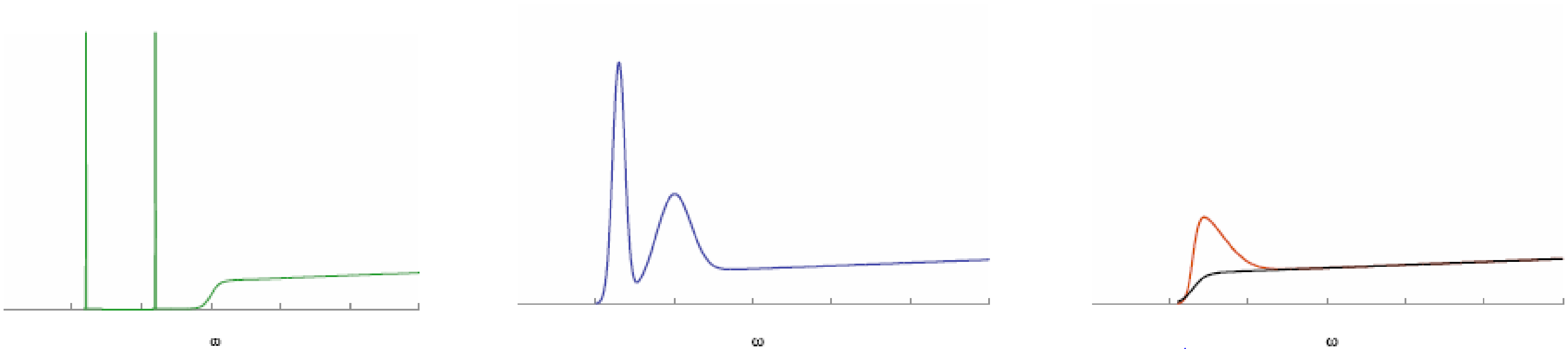


$$C(\tau,T) = \sum_x \langle O(x,\tau)O(0,0)\rangle_T \quad \longleftrightarrow \quad C(\tau,T) = \int_{-\infty}^{+\infty} d\omega \rho(\omega,T) e^{-\tau\omega}$$

Consider large $\tau$ behavior of $C(\tau, T=0)$:

$$C(\tau,T) \sim \sum_n |\langle 0|O|n\rangle|^2 e^{-M_n\tau} \simeq f_1 e^{-M_1\tau} + f_2 e^{-M_2\tau} + \dots$$

$T > 0: \quad \tau < 1/T \Rightarrow$ reconstruct $\rho(\omega,T)$

# Current-current Correlators and Transport Coefficients

$$\rho_V^{\mu\nu}(\omega) = \frac{1}{2\pi}\int_{-\infty}^{\infty} \mathrm{d}t e^{i\omega t}\int \mathrm{d}^3x \left\langle [\hat{J}^\mu(t,\vec{x}), \hat{J}^\nu(0,\vec{0})] \right\rangle_T$$

$$D_s = \lim_{\omega\to 0}\frac{1}{3\chi_2^q}\sum_i \frac{\rho_V^{ii}(\omega)}{\omega}, \quad q = u,d,s,c,b$$

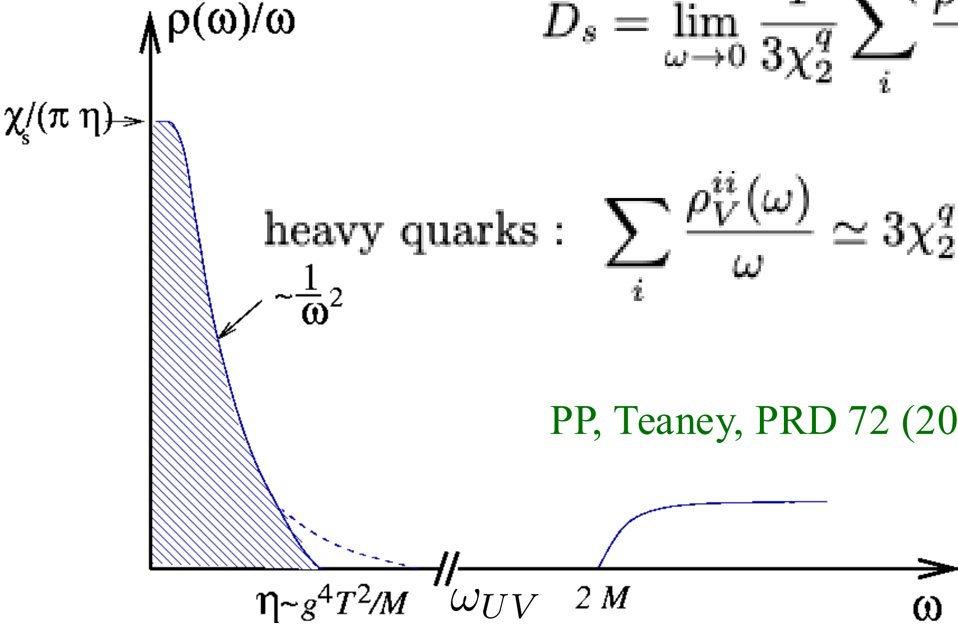


$$\text{heavy quarks}: \quad \sum_i \frac{\rho_V^{ii}(\omega)}{\omega} \simeq 3\chi_2^q \frac{T}{M}\frac{\eta}{\eta^2+\omega^2}, \quad \omega < \omega_{UV}, \quad \eta = \frac{T}{M}\frac{1}{D_s} \sim t_R^{-1}$$

$$mean\ free\ path \sim \frac{M}{T} D_s$$

PP, Teaney, PRD 72 (2006) 014508

$$\text{weak coupling}: \quad D_s \sim \frac{1}{\alpha_s^2 T}$$

$J_\mu \to T_{\mu\nu} \Rightarrow$ shear, $\eta$ and bulk, $\zeta$ viscosities which control the collective behavior and equilibration of the matter produced in heavy ion collisions

$\eta/s$ and $\zeta/s$ are small for strongly interacting QGP

Heavy ion experiment: $\eta/s \simeq 0.1 - 0.2$

very difficult to determine in LQCD

$$mean\ free\ path \sim \eta/s$$

# NRQCD meson correlators

Point correlators:

Aarts et al (FASTUM) , Kim, PP, Rothkopf

$$C_p(t) = \sum_{\mathbf{x}} \langle O_p(t,\mathbf{x}) O_p(0,\mathbf{0}) \rangle,$$

$$O_p(t,\mathbf{x}) = \chi^\dagger(t,\mathbf{x}) \Gamma \psi(t,\mathbf{x}))$$

$t = \tau / a$

| State | Irrep $\Lambda^{PC}$ | $\Gamma$ |
|---|---|---|
| $\eta_b$ | $A_1^{-+}$ | $1$ |
| $\Upsilon$ | $T_1^{--}$ | $\sigma_j$ |
| $h_b$ | $T_1^{+-}$ | $\nabla_j$ |
| $\chi_{b0}$ | $A_1^{++}$ | $\boldsymbol{\sigma} \cdot \boldsymbol{\nabla}$ |
| $\chi_{b1}$ | $T_1^{++}$ | $(\boldsymbol{\sigma} \times \boldsymbol{\nabla})_j$ |
| $\chi_{b2}$ | $T_2^{++}$ | $\sigma_j \nabla_k + \sigma_k \nabla_j$ |

Extended correlators:

$$O_p(t,\mathbf{x}) \to O(t,\mathbf{x}) = \sum_{\mathbf{r}} \Psi(\mathbf{r}) \chi^\dagger(t,\mathbf{x}) \Gamma \psi(t,\mathbf{x}+\mathbf{r}))$$

$\Psi(\mathbf{r}) \sim e^{-|\mathbf{r}|^2/\sigma^2}$
or realistic wave-function

Optimized correlators: use several different extended meson operators with realistic wave functions and form orthogonal combinations

$$O_i \to \tilde{O}_\alpha = \Omega_{\alpha j} O_j, \ \langle \tilde{O}_\alpha(t) \tilde{O}^\dagger_\beta(0) \rangle \propto \delta_{\alpha,\beta}, \ i = 1, 2, 3, \ldots$$

Mixed correlators (Bethe-Salpeter amplitudes ):

Bethe-Salpeter amplitude

$$\tilde{C}^r_\alpha(t) = \sum_{\mathbf{x}} \langle O^r_{qq}(t,\mathbf{x}) \tilde{O}_\alpha(0,\mathbf{0}) \rangle \sim \phi_\alpha(r) e^{-E_\alpha t}, \ t \to \infty$$

$$O^r_{qq}(t,\mathbf{x}) = \chi^\dagger(t,\mathbf{x}) \Gamma \psi(t,\mathbf{x}+\mathbf{r}))$$

# Point operators vs. extended operators

Larsen, Meinel, Mukherjee, PP, PRD100 (2019) 074506

$$M_{\text{eff}}(\tau) = \frac{1}{a}\ln[C_\alpha(\tau)/C_\alpha(\tau+a)]$$

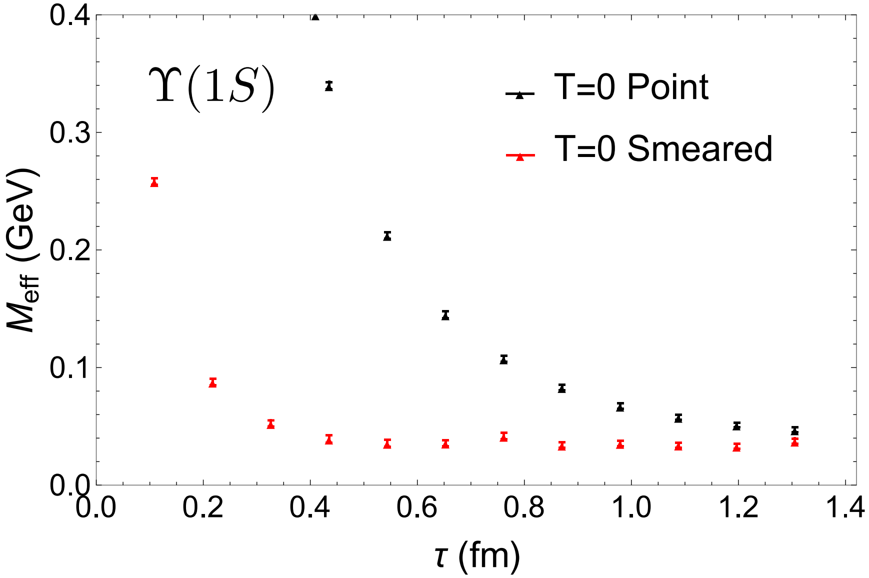


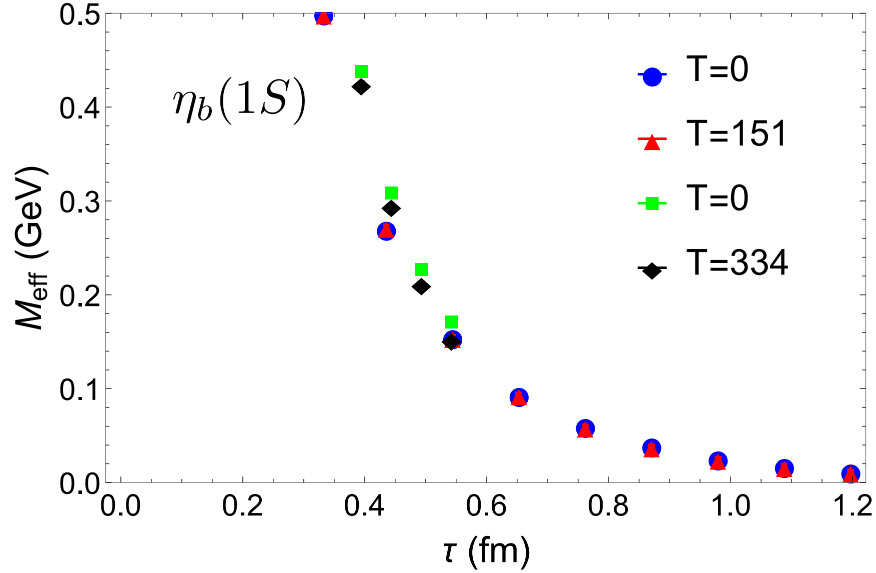


- The effective masses of point correlators do not show a plateau for $\tau < 1.2$ fm and have very small temperature dependence
- The small $\tau$ behavior of the effective masses is well described by perturbation theory for P-wave bottomonia
- The correlators of extended operators approach a plateau for $\tau < 1$ fm.

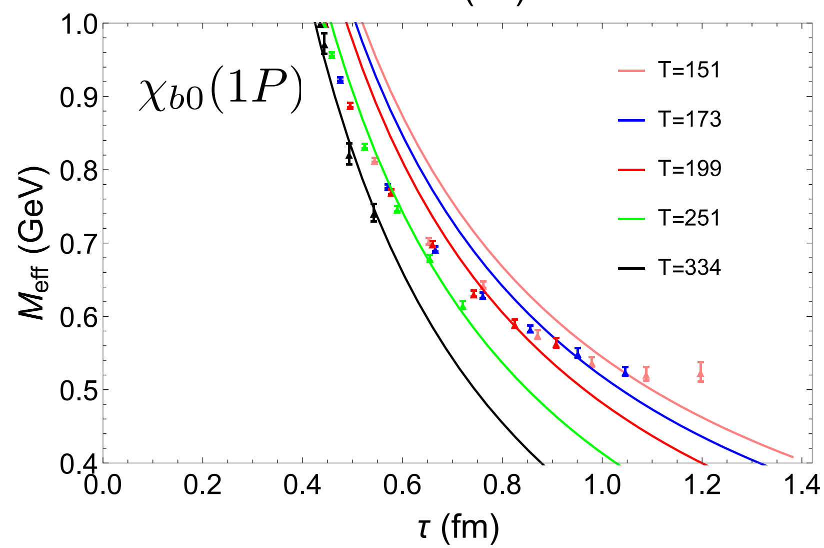

# Correlators of Optimized Meson Operators at T=0

HISQ, $a = 0.109,\ 0.095,\ 0.083,\ 0.066,\ 0.060,\ 0.049$ fm, $48^3 \times 12$

Larsen, Meinel, Mukherjee, PP, PLB 800 (2020) 135119

$$M_{\rm eff}(\tau) = \frac{1}{a} \ln[C_\alpha(\tau)/C_\alpha(\tau+a)]$$

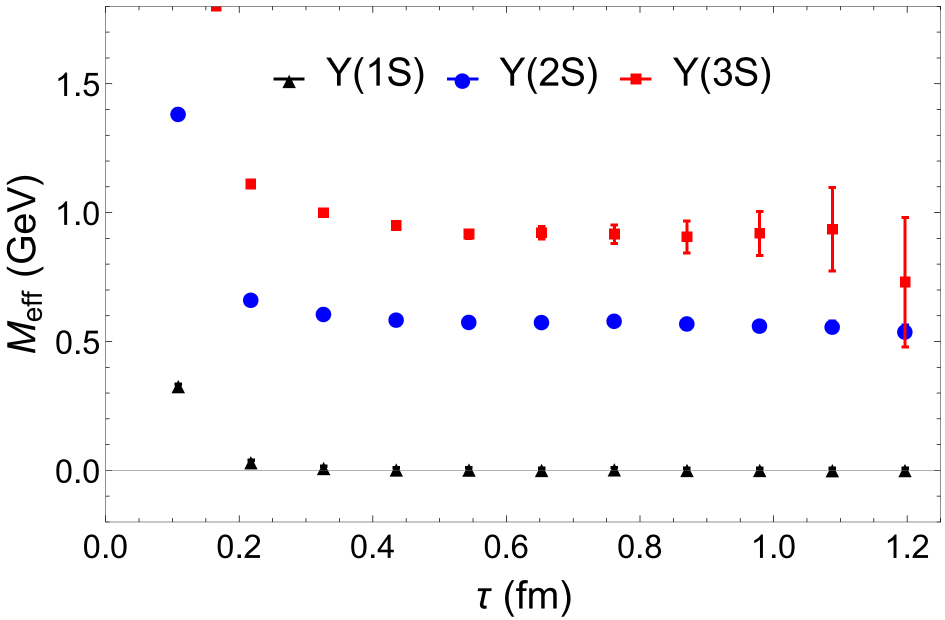


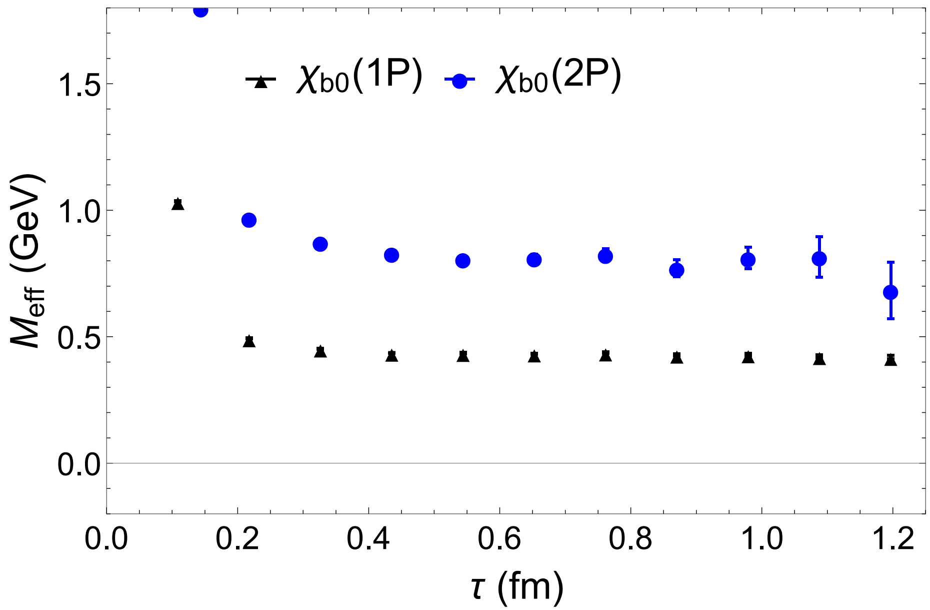


$$C_\alpha(\tau,T) = \int_{-\infty}^{\infty} d\omega \rho_\alpha(\omega,T) e^{-\omega\tau}$$

$$\rho_\alpha(\omega,T) = \rho_\alpha^{\rm med}(\omega,T) + \rho_\alpha^{\rm high}(\omega)$$

$$\rho_\alpha^{\rm med}(\omega,T=0) = A_\alpha \delta(\omega - M_\alpha) \Rightarrow C_\alpha(\tau,T=0) = A_\alpha e^{-M_\alpha\tau} + C_\alpha^{\rm high}(\tau)$$

Determine $A_\alpha, M_\alpha$ from single exponential fit for $\tau > 0.6$fm and then $C_\alpha^{\rm high}(\tau)$

# Correlators of Extended Meson Operators at T>0

Larsen, Meinel, Mukherjee, PP, PLB 800 (2020) 135119

Ding, Huang, Larsen, Meinel, Mukherjee, PP, Tang JHEP 05 (2025) 149

$$C_\alpha^{\rm sub}(\tau,T)=C_\alpha(\tau,T)-C_\alpha^{\rm high}(\tau)\Rightarrow aM_{\rm eff}^{\rm sub}(\tau,T)=\ln\left(C_\alpha^{\rm sub}(\tau,T)/C_\alpha^{\rm sub}(\tau+a,T)\right)$$

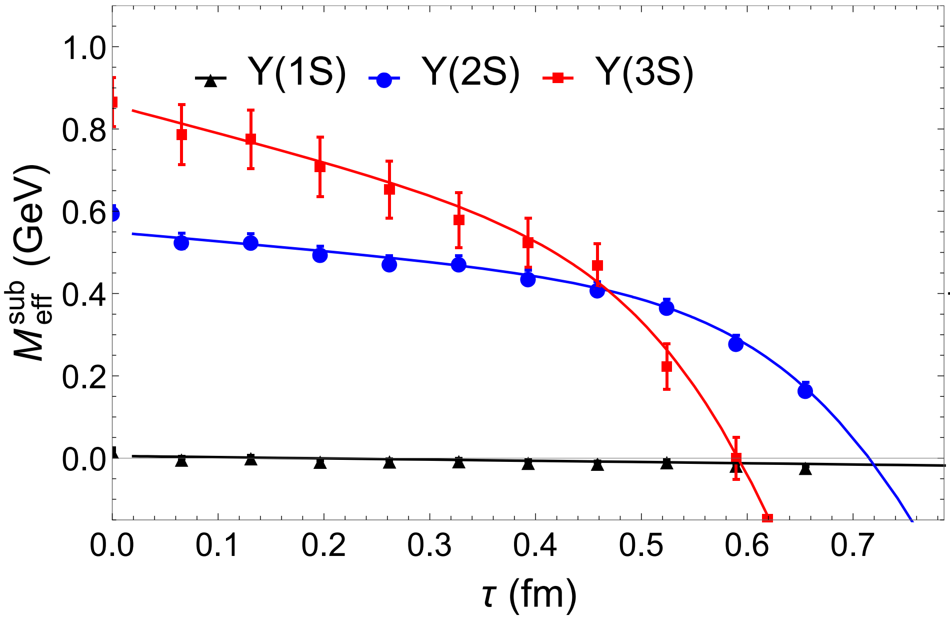


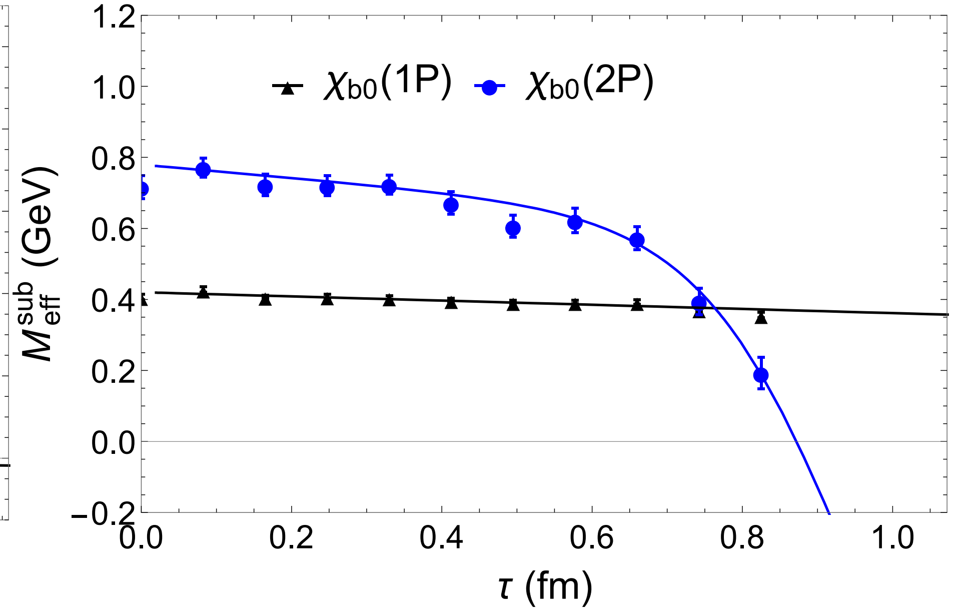


Fit $M_{\rm eff}^{\rm sub}(\tau,T)$ using a simple Ansatz:

$$\rho_\alpha^{\rm med}(\omega,T)=A_\alpha^{\rm low}(T)\,\delta\left(\omega-\omega_\alpha^{\rm low}(T)\right)+A_\alpha(T)\frac{1}{\pi}\frac{\Gamma_\alpha(\omega,T)}{(\omega-M_\alpha(T))^2+\Gamma_\alpha^2(\omega,T)}$$

Low energy tail

$\Gamma(\omega\simeq M_\alpha,T)\simeq\Gamma_0$, and $\Gamma(\omega,T)\to 0$ for $|\omega-M_\alpha(T)|\gg\Gamma_0$

$\Rightarrow M_\alpha(T),\Gamma_\alpha(T)$

# Thermal mass shift of bottomonium

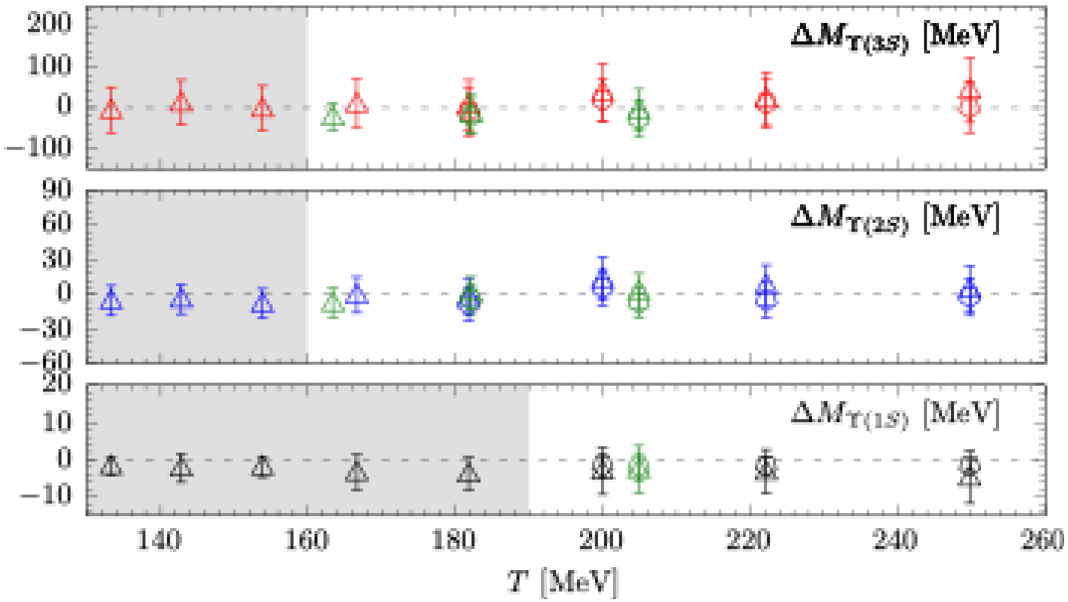


$$\Delta M_\alpha(T) = M_\alpha(T) - M_\alpha(T=0)$$

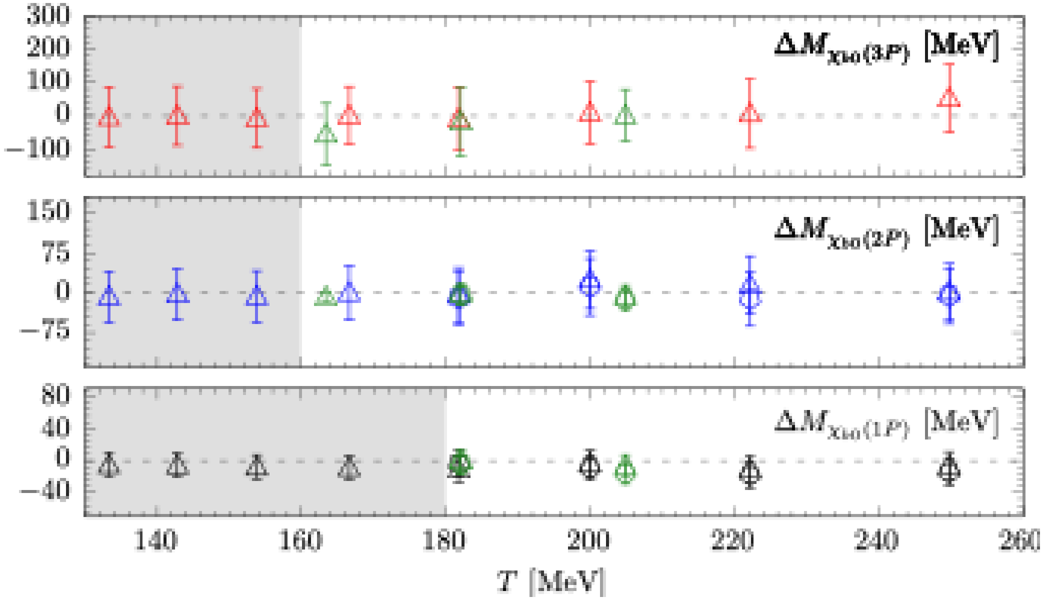


No shift in the bottomonium masses
=>. very small screening,
Ding, Huang, Larsen, Meinel, Mukherjee, PP, Tang JHEP 05 (2025) 149

# Thermal width of bottomonium

Ding, Huang, Larsen, Meinel, Mukherjee, PP, Tang JHEP 05 (2025) 149

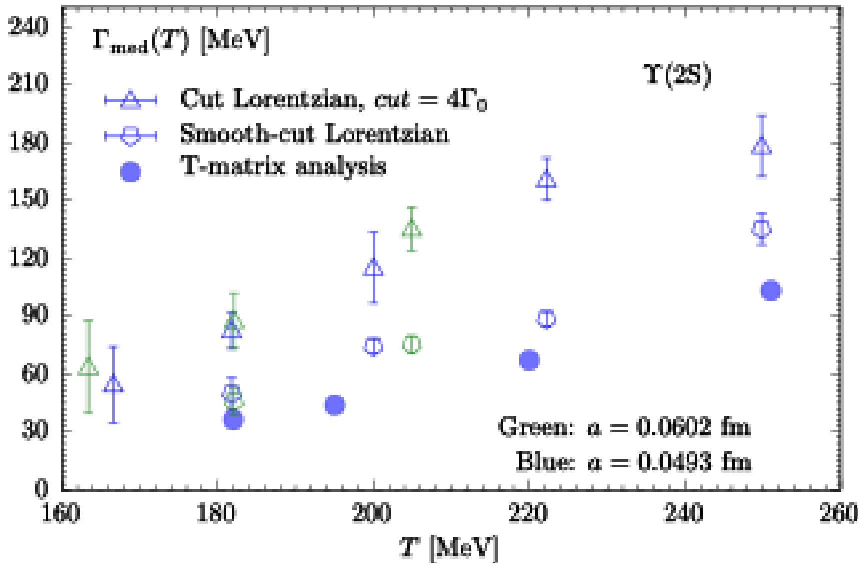


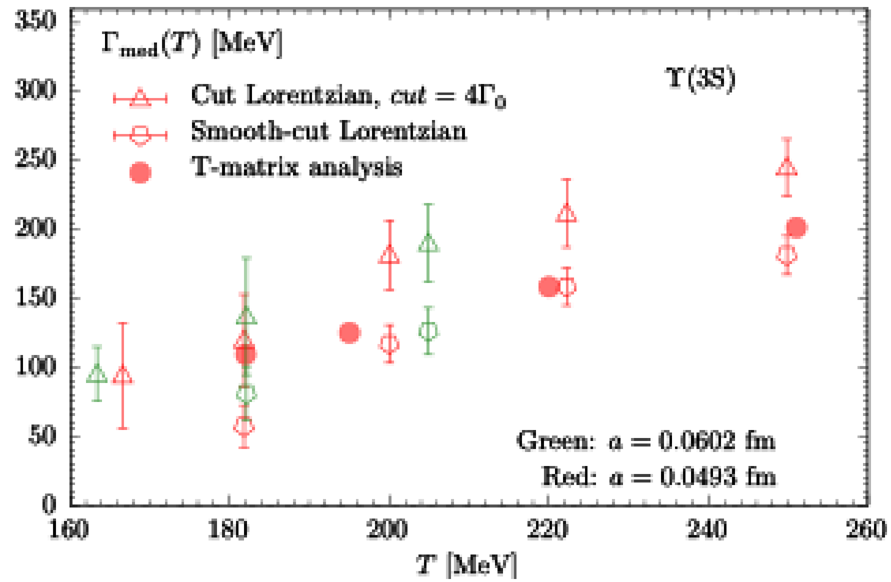


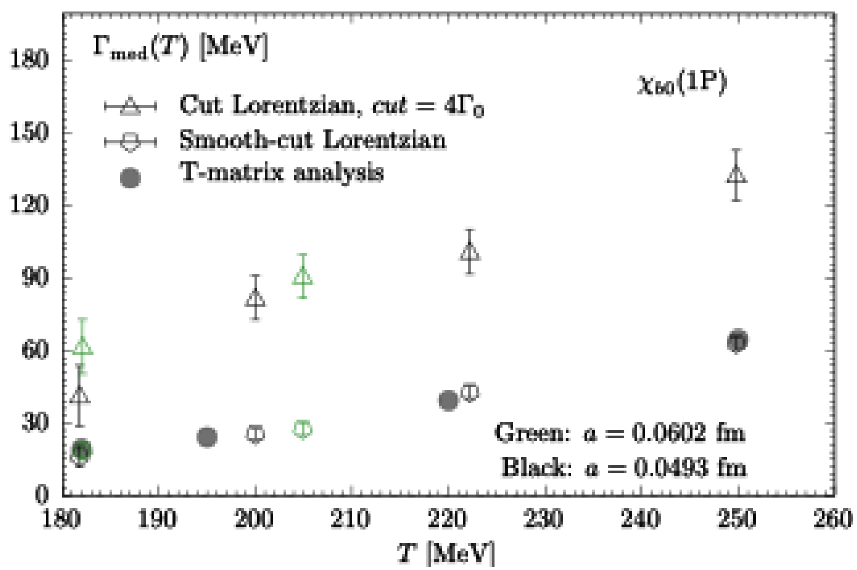


Significant thermal width for all bottomonium states that increases with $T$

Some sensitivity of the width to the form of the spectral peak

# Quark anti-quark potential at T>0

Conjecture, Matsui and Satz, PLB 178 (1986) 416 $-\frac{4}{3}\frac{\alpha_s}{r} + \sigma r \to -\frac{4}{3}\frac{\alpha_s}{r} e^{-m_D r}, T > T_c$

Extending pNRQCD to *T>0*: the potential is complex, the real part can have thermal correction but is not necessarily screened, except when $r \sim 1/m_D$

Based on weak coupling

Laine, Philipsen, Romatschke, Tassler, JHEP 03 (2006) 054
Brambilla, Ghiglieri, PP, Vairo, PRD 78 (2008) 014017

Calculate the potential non-perturbatively on the lattice by considering Wislon loops of size $r \times \tau$ at $T>0$

$$W(r,\tau,T) = \int_{-\infty}^{\infty} \rho_r(\omega,T) e^{-\omega\tau}$$

If potential at $T > 0$ exists the $\rho_r(\omega,T)$ should have a well define peak at $\omega \simeq \mathrm{Re}V(r,T)$, and the width of the peak is $\mathrm{Im}V(r,T)$

Rothkopf, Hatsuda, Sasaki, PRL 108 (2012) 162001

Challenge: reconstruct $\rho_r(\omega,T) \Rightarrow$ use the same approach as for reconstruction of the NRQCD bottomonium spectral functions

# Details of the lattice calculations of the potential

HISQ action, $T = 153 - 352$ MeV  Bazavov et al (HotQCD), PRD 109 (2024) 074504

$a = 0.028$ fm, $m_l = m_s/5$, $(m_\pi = 320$ MeV$)$, $96^3 \times N_\tau$, $N_\tau = 56,\ 36,\ 32,\ 28,\ 24,\ 20$

$a = 0.040$ fm, $m_l = m_s/20$, $(m_\pi = 160$ MeV$)$, $64^3 \times N_\tau$, $N_\tau = 64,\ 32,\ 30,\ 28,\ 26,\ 24,\ 22,\ 20,\ 18,\ 16$

$a = 0.049$ fm, $m_l = m_s/20$, $(m_\pi = 160$ MeV$)$, $64^3 \times N_\tau$, $N_\tau = 64,\ 26,\ 24,\ 22,\ 20,\ 18,\ 16$

Calculate correlation functions of temporal Wilson line instead of Wilson loops (better signal)

Gradient (Zeuthen) flow for noise reduction:

$$A_\mu(x) \to B_\mu(\tau_F, x)$$

$$B_\mu(0, x) = A_\mu(x)$$

$$\partial_{\tau_F} B_\mu(\tau_F, x) = -g_0^2 \frac{\delta S_{\rm YM}[B]}{\delta B_\mu(\tau_F, x)}$$

Gauge fields are smeared in the radius $\sqrt{8\tau_F}$

$$M_{eff}(r, \tau, T) = -\partial_\tau \log(W(\tau, r, T)) \simeq \frac{1}{a} \ln \frac{W(r, \tau, T)}{W(r, \tau + a, T)}$$

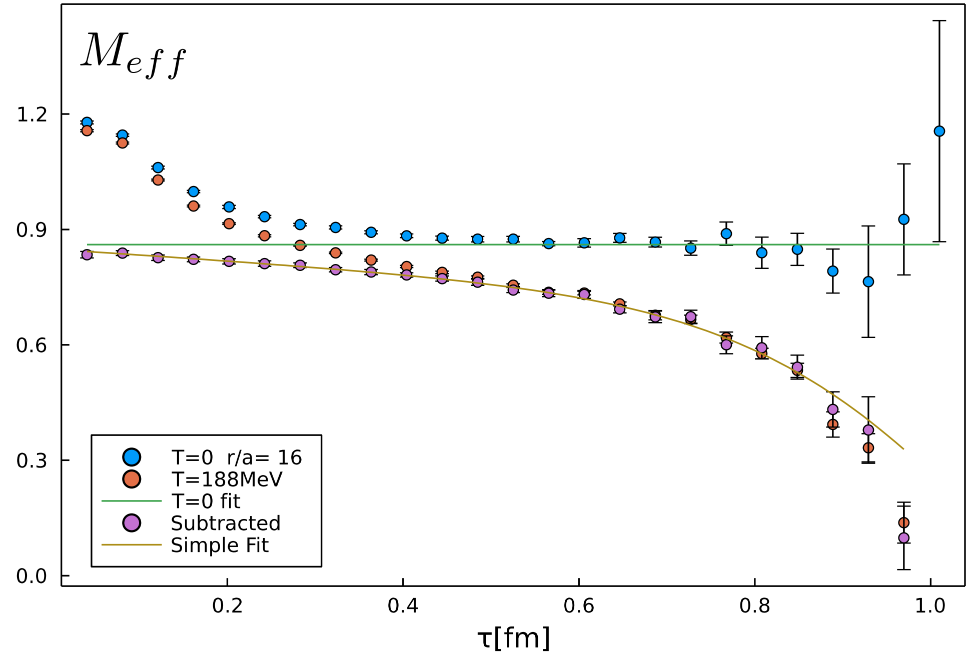


$\sqrt{8\tau_F}T = 0.04 - 0.05$

# Model spectral function and the complex potential

$$\rho_r^{peak}(\omega,T)=\frac{A}{\pi}\frac{\Gamma(\omega,r,T)}{(\omega-\mathrm{Re}V(r,T))^2+\Gamma^2(\omega,r,T)}. \qquad \rho_r^{tail}(\omega,T)=A^{tail}\delta(\omega-E^{tail})$$

$$\Gamma(\omega,r,T)=\begin{cases}\Gamma_0(r,T) & -2\Gamma_0<\omega<2\Gamma_0\\ 0 & n \text{ otherwise}\end{cases}$$

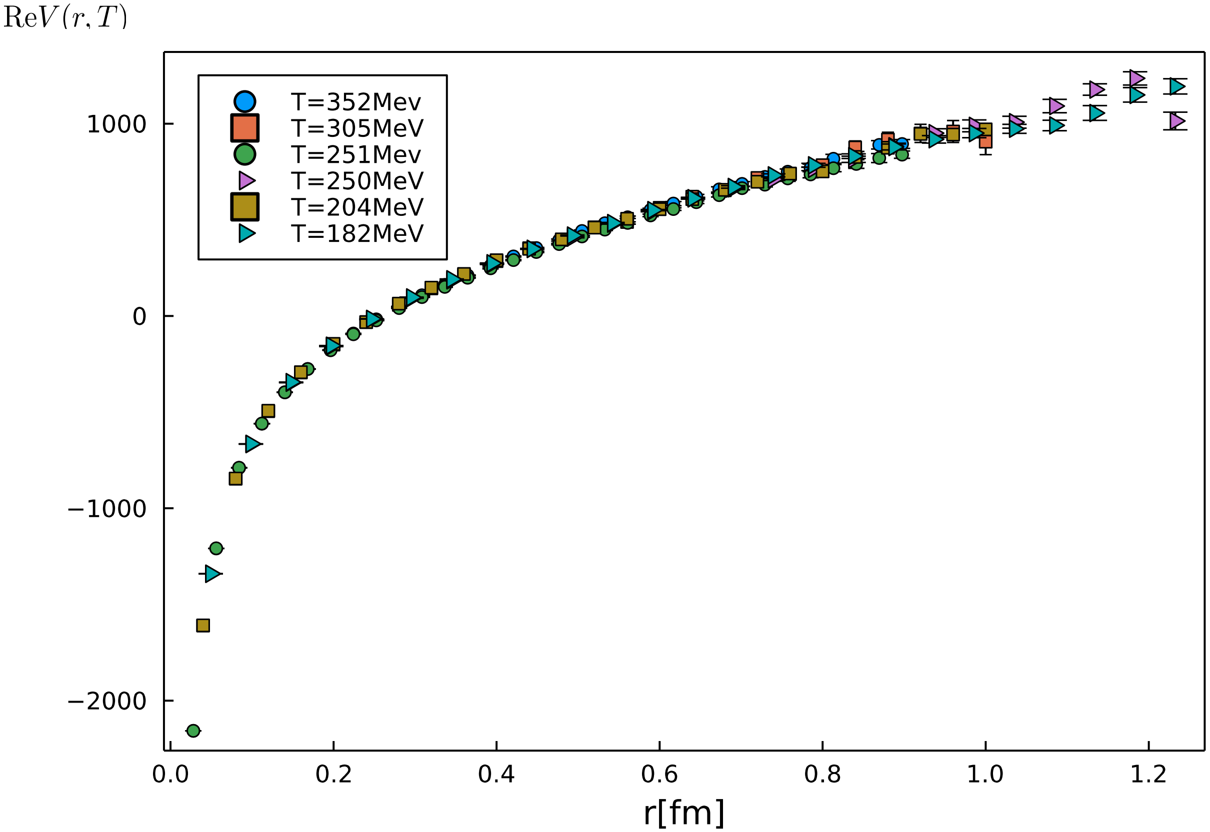


$\mathrm{Re}V(r,T)$ shows only tiny temperature dependence and no hint of screening !

Bazavov et al (HotQCD), PRD 109 (2024) 074504

The same result if $\rho_r^{peak}(\omega,T)\sim\exp(-(\omega-\mathrm{Re}V(r,T))^2/(\mathrm{Im}V(r,T))^2)$

# Imaginary part of the potential

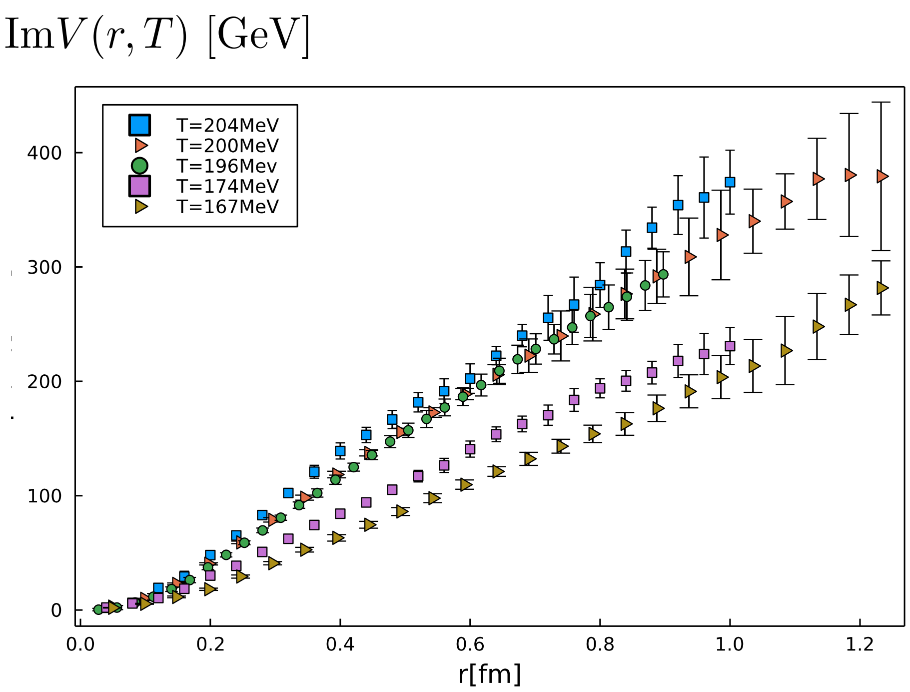


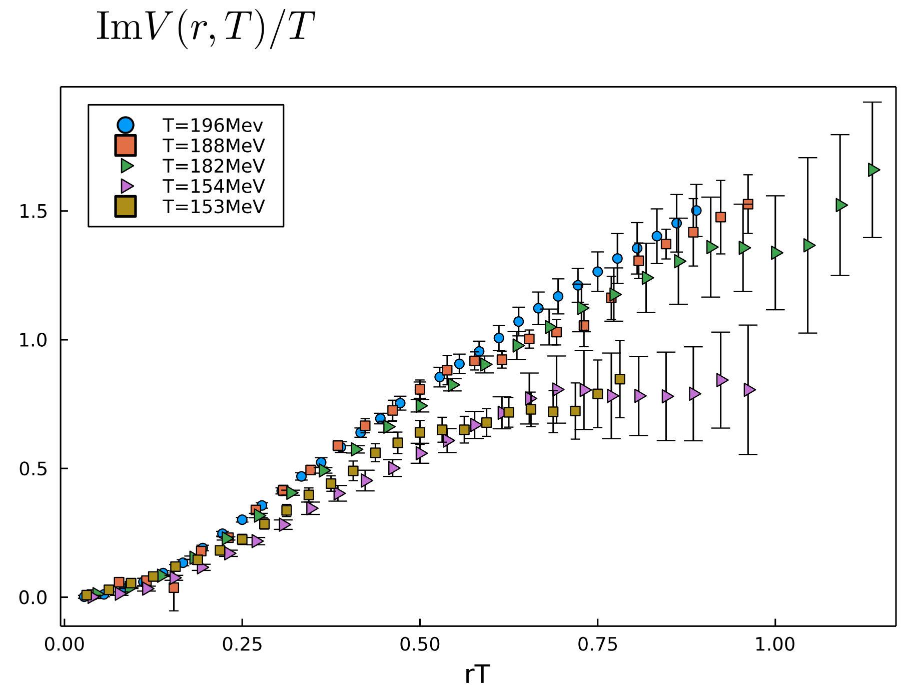


circles: $a = 0.028$ fm, squares: $a = 0.040$ fm, triangles: $a = 0.049$ fm

$\mathrm{Im}V(r,T)$ increases with increasing temperature and distance

No apparent quark mass effects for $T > 196$ MeV

No apparent cutoff effects

Bazavov et al (HotQCD), PRD 109 (2024) 074504

# Hadron Gas of charm hadrons and Deconfinement of charm

$$\chi_{nml}^{XYC} = T^{m+n+l} \frac{\partial^{n+m+l} p(T, \mu_X, \mu_Y, \mu_C)/T^4}{\partial \mu_X^n \partial \mu_Y^m \partial \mu_C^l}$$

Bazavov et al, PLB 737 ('14) 210

S. Mukherjee, PP, S. Sharma, PRD93 (2016) 014502;
HotQCD, PLB 850 (2024) 138520, PRD 112 (2025) 034509

$m_c \gg T$ ⇨ only |*C*|=*1* sector contributes

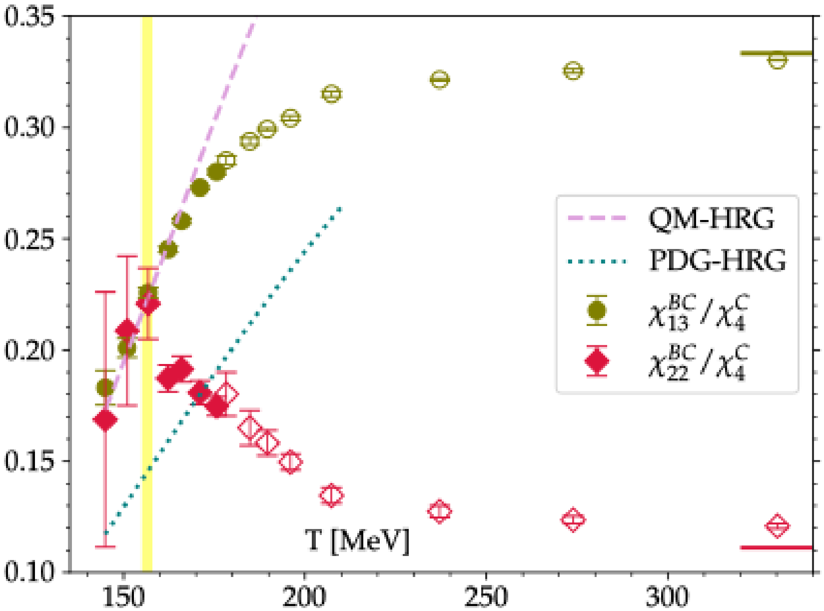


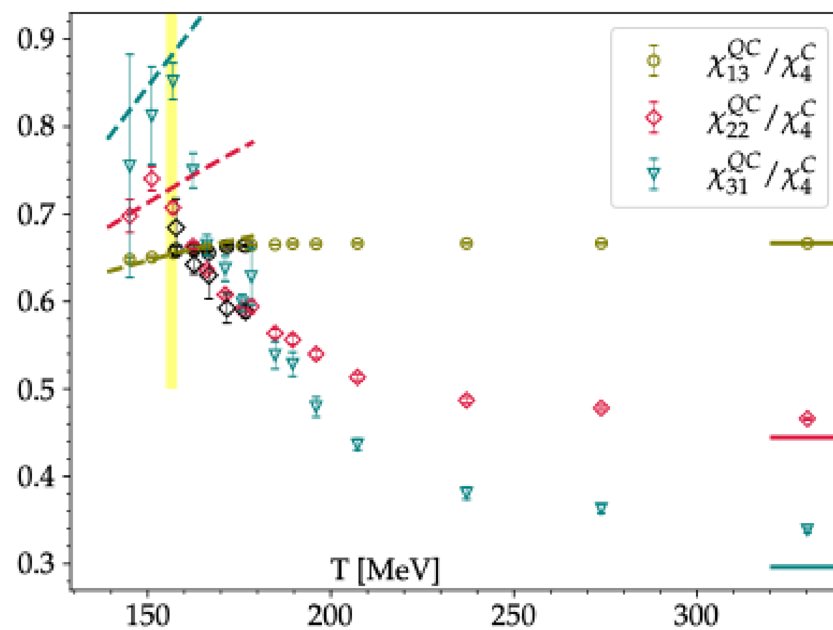


In the hadronic phase all *BC*-correlations are the same !

Hadronic description breaks down just above $T_c$
⇒ open charn deconfines above $T_c$

The charm baryon spectrum is not well known (only few states in PDG), HRG works only if the "missing" states from quark model are included

# Quasi-particle model for charm degrees of freedom

Charm dof are good quasi-particles at all $T$ because $M_c >> T$ and Boltzmann approximation holds

$$p^C(T,\mu_B,\mu_c) = p_q^C(T)\cosh(\hat{\mu}_C + \hat{\mu}_B/3) + p_B^C(T)\cosh(\hat{\mu}_C + \hat{\mu}_B) + p_M^C(T)\cosh(\hat{\mu}_C)$$

$$\chi_2^C,\ \chi_{13}^{BC},\ \chi_{22}^{BC} \Rightarrow p_q^C(T), p_M^C(T), p_B^C(T) \qquad \hat{\mu}_X = \mu_X/T$$

Partial meson and baryon pressures described by HRG at $T_c$ and dominate the charm pressure then drop gradually, charm quark only dominant dof at $T>200$ MeV or $\varepsilon > 6$ GeV/fm$^3$

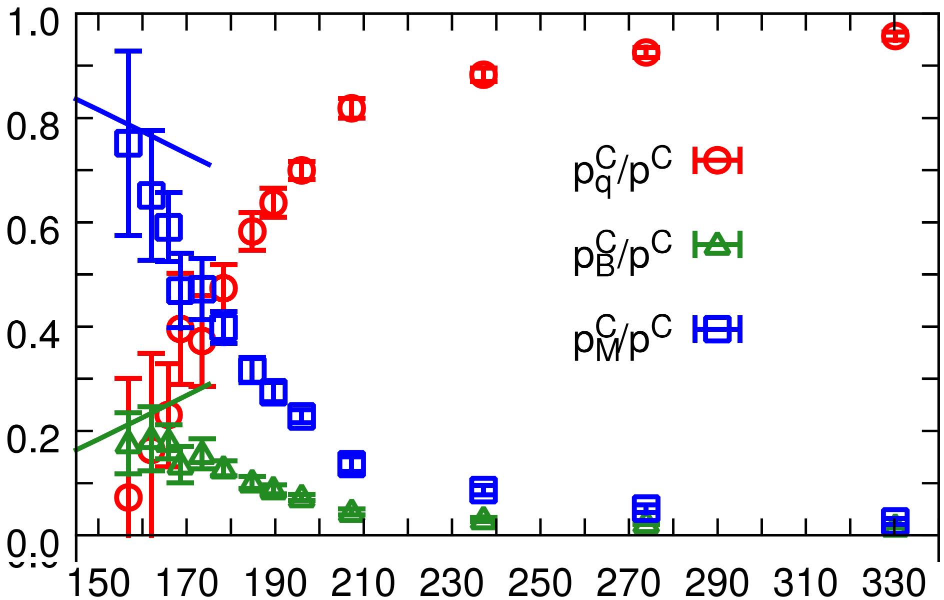


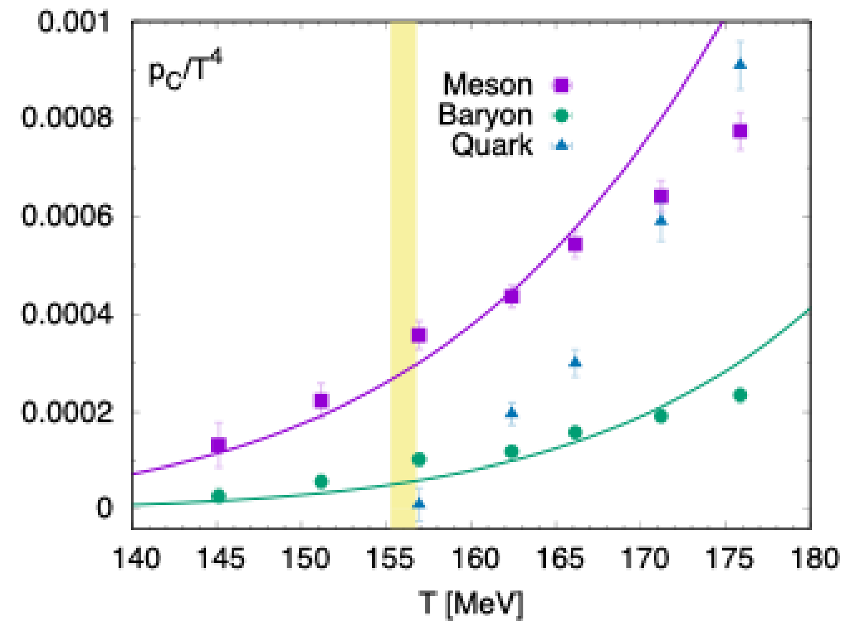


S. Mukherjee, PP, S. Sharma, PRD93 (2016) 014502;
HotQCD, PLB 850 (2024) 138520, PRD 112 (2025) 034509

# Heavy quark diffusion and lattice QCD

$$\partial_t p_i = -\eta p_i + f_i(t),$$

$$\langle f_i(t) f_j(t') \rangle = \kappa \delta_{ij} \delta(t - t')$$

$$D_s = \frac{T}{M}\frac{1}{\eta} = \frac{2T^2}{\kappa}\frac{\langle \mathbf{p}^2 \rangle}{3MT}, \quad \langle \mathbf{p}^2 \rangle = \frac{3\kappa}{2\eta}$$

$$\langle f_i(t) f_j(t) \rangle = \langle E_i(t) E_j(t') \rangle + \frac{1}{3}\langle \mathbf{v}^2 \rangle \langle \delta_{ij} B_k(t) B_k(t') - B_i(t') B_j(t) \rangle \qquad \langle \mathbf{v}^2 \rangle = \frac{3T}{M}$$

$$t \to i\tau$$

Casalderrey-Solana, Teaney, PRD 74 (2006) 085012; Caron-Huot, Laine, Moore, JHEP 0904 ('09) 053

Bouttefeux, Laine, JHEP 12 (2020) 150

$$G_E(\tau) = -\frac{1}{3}\sum_{i=1}^{3} \frac{\left\langle \mathrm{Re}\mathrm{Tr}\left[U(\beta,\tau)\, gE_i(\tau,\vec{0})\, U(\tau,0)\, gE_i(0,\vec{0})\right]\right\rangle}{\left\langle \mathrm{Re}\mathrm{Tr}[U(\beta,0)]\right\rangle} \qquad \kappa_E = \lim_{\omega\to 0}\frac{2T}{\omega}\rho_E(\omega)$$

$$G_B(\tau) = -\frac{1}{3}\sum_{i=1}^{3} \frac{\left\langle \mathrm{Re}\mathrm{Tr}\left[U(\beta,\tau)\, gB_i(\tau,\vec{0})\, U(\tau,0)\, gB_i(0,\vec{0})\right]\right\rangle}{\left\langle \mathrm{Re}\mathrm{Tr}[U(\beta,0)]\right\rangle} \qquad \kappa_B = \lim_{\omega\to 0}\frac{2T}{\omega}\rho_B(\omega)$$

$$G_{E,B}(\tau) = \int_0^\infty \frac{\mathrm{d}\omega}{\pi}\rho_{E,B}(\omega)\frac{\cosh\left(\tau - \frac{1}{2T}\right)\omega}{\sinh\frac{\omega}{2T}}$$

$$\kappa = \kappa_E + \frac{2}{3}\langle \mathbf{v}^2 \rangle \kappa_B$$

# Extracting momentum diffusion coefficient from the lattice

Challenge 1: obtain precise results for chromo-electric and chromo-magnetic (very noisy)

⇒ Noise reduction via multi-level algorithm, applicable to quenched QCD (pure glue plasma)

⇒ Noise reduction by gradient flow method (new development !) , also applicable in full QCD

Challenge 2: reconstruct the spectral function from the Euclidean time lattice correlator

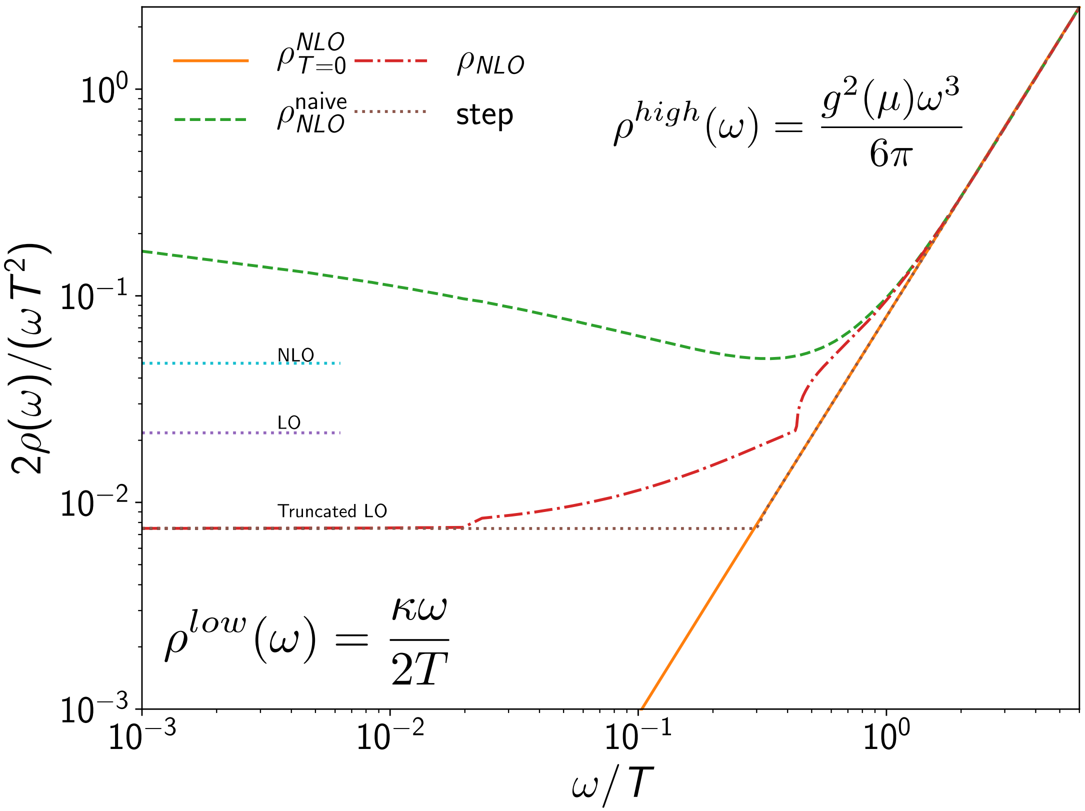


⇒ use known large and small energy behavior of the spectral

Parameterize $\rho(\omega, T)$ as smooth interpolation between $\rho^{low}(\omega, T)$ and $\rho^{high}(\omega)$, and treat $\kappa$ as well as the additional nuisance parameters of interpolation as fit parameters

Brambilla et al (TUMQCD), PRD 102 (2020) 0740503

# Extracting momentum diffusion coefficient from the lattice

2+1 flavor QCD with $m_l = m_s/5$ ($m_\pi = 320$ MeV), $T = 195 - 354$ MeV, $96^3 \times N_\tau$ lattices with $N_\tau = 36,\ 32,\ 28,\ 24,\ 20$; additional $64^3 \times N_\tau$ lattices with $N_\tau = 20,\ 22,\ 24 \Rightarrow 3$ lattice spacings at each $T$; Gradient flow for noise reduction

Altenkort et al (HotQCD), PRL 130 (2023) 231902

Symanzik gauge action and Zeuthen flow

Gauge fields are smeared in the radius $\sqrt{8\tau_F}$

$$a < \sqrt{8\tau_F} < \tau/3$$

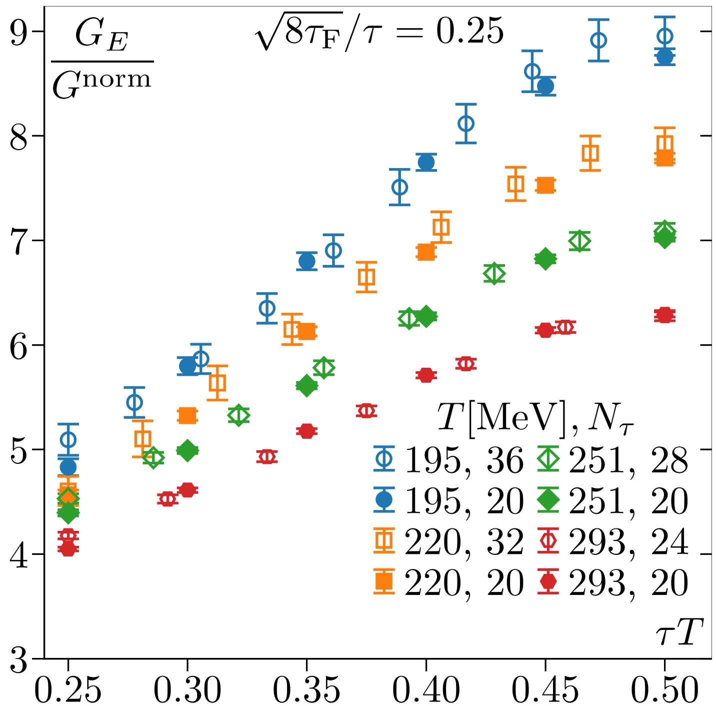


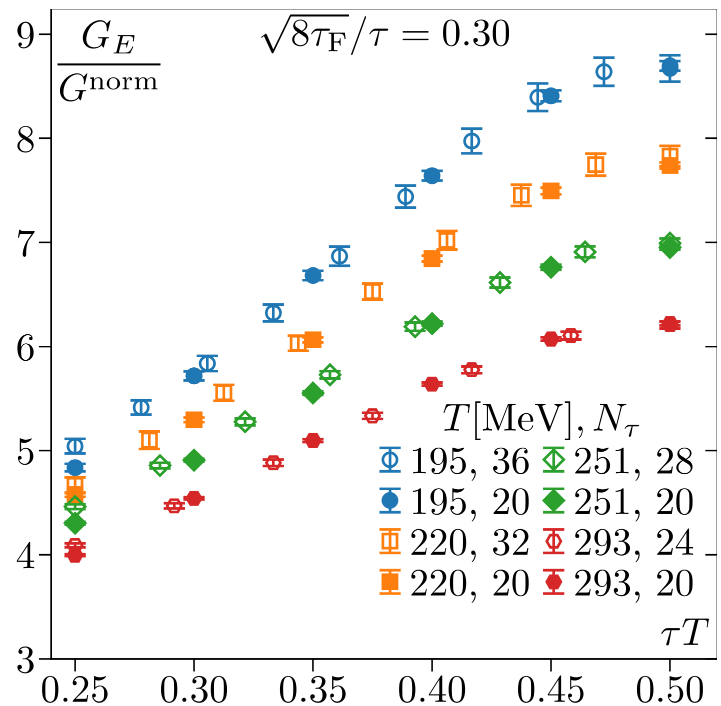


We see small cutoff effects thanks improved actions

# Analysis and modeling the chromo-electric correlator

Analysis of the chromo-electric correlator:

- Extrapolate the lattice results on the chromo-electric correlator to the continuum limit
- Perform the zero flow time extrapolation

Altenkort et al (HotQCD), PRL 130 (2023) 231902

Fits to model spectral function:

$$\rho^{low}(\omega,T)=\frac{\kappa\omega}{2T} \qquad \rho^{high}(\omega)=\rho^{LO,NLO}(\omega)$$

$$\rho^{max}(\omega,T)=max(\rho^{low}(\omega,T),\rho^{high}(\omega))$$

$$\rho^{smax}(\omega,T)=\sqrt{(\rho^{low})^2+(\rho^{high})^2}$$

$$\rho^{pow}(\omega,T)=\rho^{low}(\omega,T),\ \omega\le\omega_{IR}$$

$$\rho^{pow}(\omega,T)=A\omega^{\alpha},\ \omega_{IR}<\omega<\omega_{UV}$$

$$\rho^{pow}(\omega)=\rho^{high}(\omega),\ \omega\ge\omega_{UV}$$

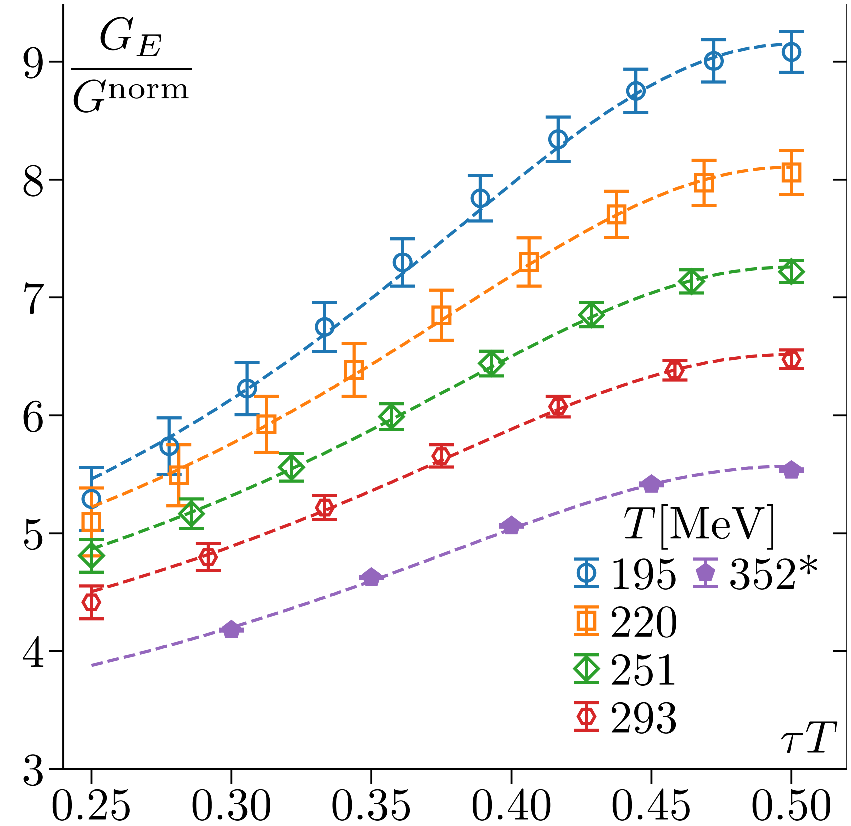

# Heavy quark diffusion coefficient in QCD

- $D_s$ has significant temperature dependence
- $D_s$ is significantly smaller in 2+1 flavor QCD than in quenched QCD and is close to the AdS/CFT limit around the crossover temperature, but compatible with NLO perturbative result at high temperature

$$D_s = \frac{2T^2}{\kappa_E + 2\kappa_B\langle \mathbf{v}^2\rangle/3} \cdot \frac{\langle p^2\rangle}{3MT}$$

HotQCD, PRL 130 (2023) 231902
PRL 132 (2024) 051902, arXiV:2506.11958

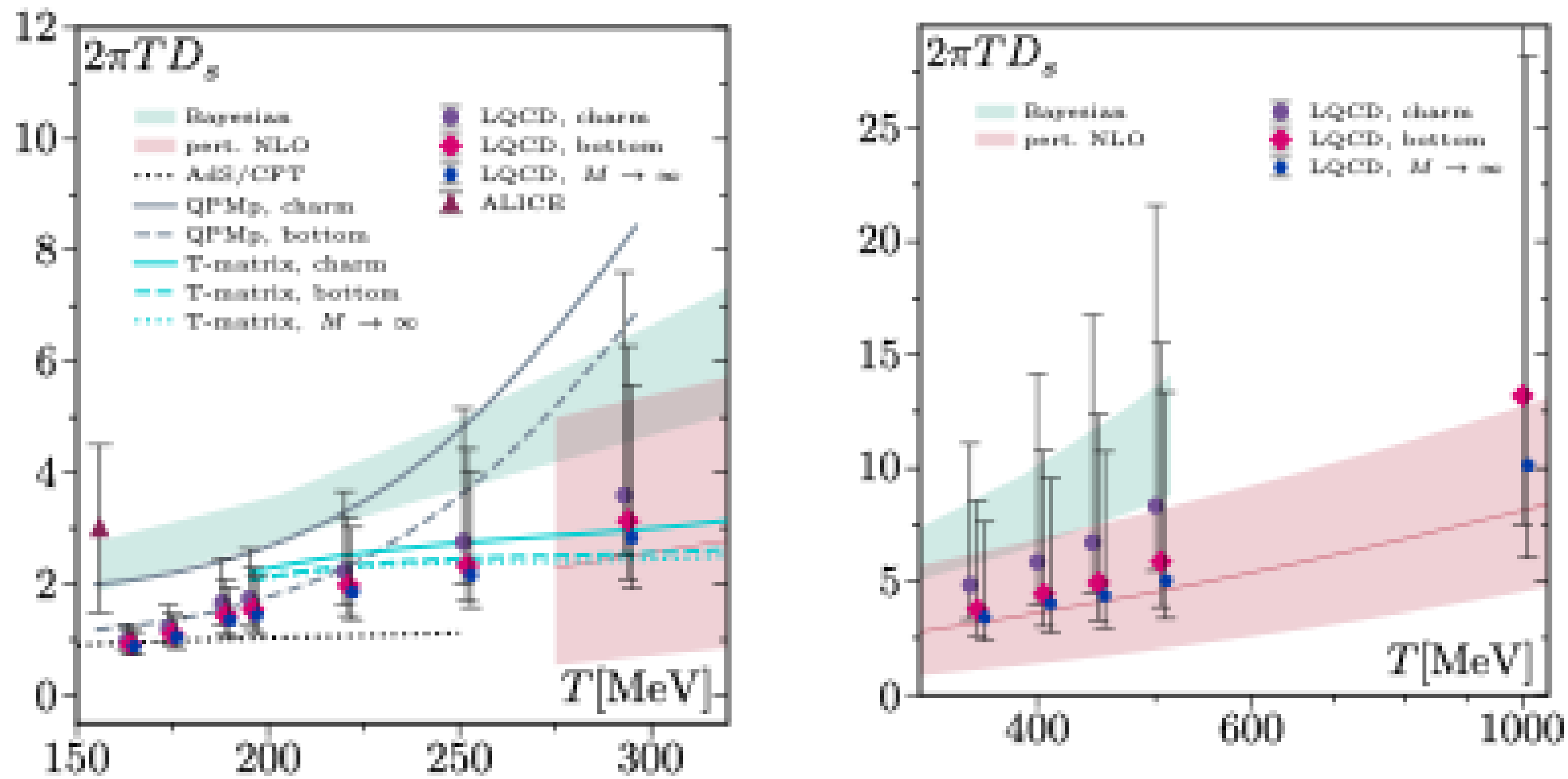

# Summary

- No significant thermal modification of bottomonium masses have been found in contrast with the expectations based on potential models with screened potential
- Lattice calculations confirm the existence of the imaginary part of the potential; There is no evidence for the screening of the real part of the potential $\Rightarrow$ Matsui and Satz picture is not correct, quarkonium melting is not related to color screening
- Quarkonia have a significant thermal width above the crossover temperature, which increases with increasing temperature
- To understand thermodynamics of the charm quarks it is necessary to include additional ("missing") charm baryons that predicted by quark models but are not in PDG; Charm meson and baryon like excitations exist above $T_c$
- Full QCD calculation of the heavy quark diffusion coefficient are available now and indicate that $D_s$ is smaller than in quenched QCD, and close to the AdS/CFT bound around the crossover temperature, but compatible with NLO perturbative calculations at high temperatures

# Back-up Static quark anti-quark free energy in 2+1f QCD

HISQ action, $24^3 \times 6$, $16^3 \times 4$ (high T) lattices, $m_\pi \simeq 160$ MeV

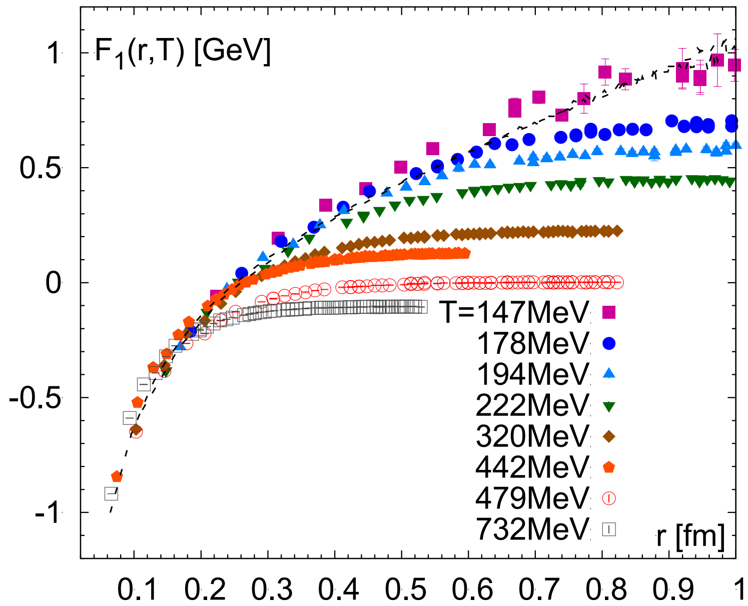


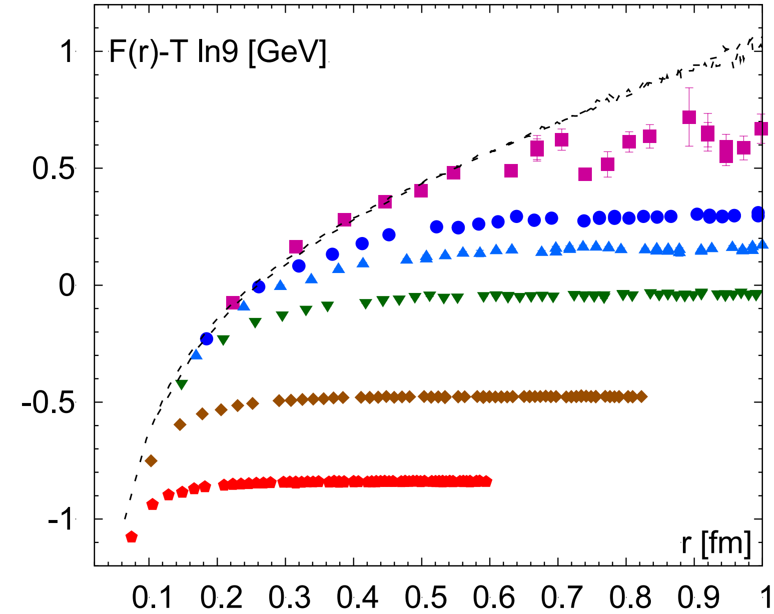


• The strong *T*-dependence for *T<200* MeV is not necessarily related to color screening

• The free energy has much stronger *T*-dependence than the singlet free energy due to the octet contribution

• At high T the temperature dependence of the free energy can be entirely understood in terms of $F_1$ and Casimir scaling $F_1=-8\ F_8$

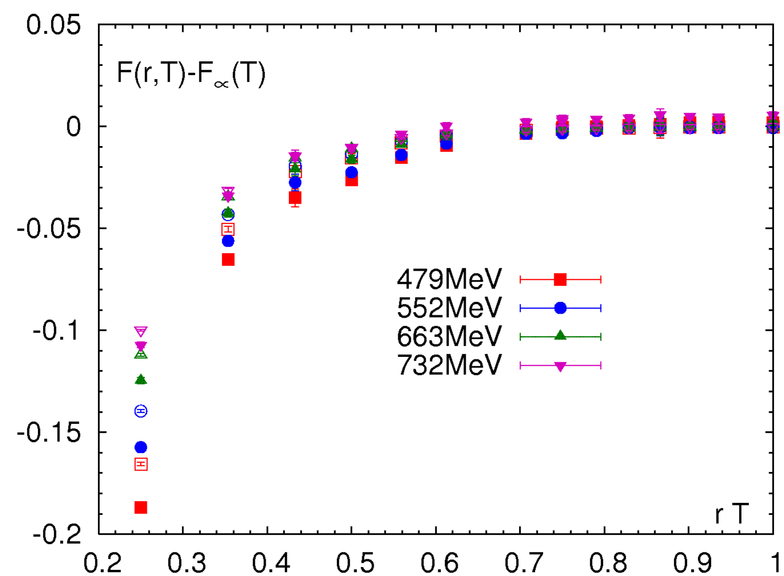

# Back-up: NRQCD on the Lattice

Advantages: No large cutoff effects $\sim aM_b$, large $\tau$ range for $T > 0$

Inverse lattice spacing provides a natural UV cutoff for NRQCD, provided $a^{-1} \leq 2M_Q$ (lattices cannot be too fine)

Quark propagators are obtained as initial value problem:

$$G_\psi(\mathbf{x},t) = \langle \psi(\mathbf{x},t)\, \psi^\dagger(\mathbf{0},0)\rangle \qquad G_\chi(\mathbf{x},t) = -G_\psi^\dagger(\mathbf{x},t)$$

$$G_\psi(t) = K(t) G_\psi(t-1),$$

$$K(t) = \left(1 - \frac{a\delta H|_t}{2}\right)\left(1 - \frac{aH_0|_t}{2n}\right)^n U_4^\dagger(t) \times \left(1 - \frac{aH_0|_{t-1}}{2n}\right)^n \left(1 - \frac{a\delta H|_{t-1}}{2}\right),$$

$$t = \tau/a,\ H_0 = \frac{-\Delta^{(2)}}{2M_b},\quad \delta H \sim v^4,\ v^6(\text{ spin} - \text{dep.})$$

@ Tree level

Meinel, PRD 82 (2010) 114502

masses are only defined up to *a*-dependent shift: $M_{\Upsilon(1S)} = E_{\Upsilon(1S)} + C_{\text{shift}}(a)$

Use kinetic mass instead: $E_{\Upsilon(1S)}(p) = E_{\Upsilon(1S)} + C_{\text{shift}}(a) + \frac{p^2}{2M^{kin}_{\Upsilon(1S)}}$

Tune $M_b$ such that $M^{kin}_{\Upsilon(1S)} = M^{PDG}_{\Upsilon(1S)}$

# Back-up: Optimized Meson Operators

$O_i(\mathbf{x},t) = \sum_{\mathbf{r}} \Psi_i(\mathbf{r})\chi^\dagger(\mathbf{x}+\mathbf{r},t)\Gamma\psi(\mathbf{x},t)$ $\Psi_i(\mathbf{r})$ from potential model with Cornell potential

Meinel, PRD 82 (2010) 114502

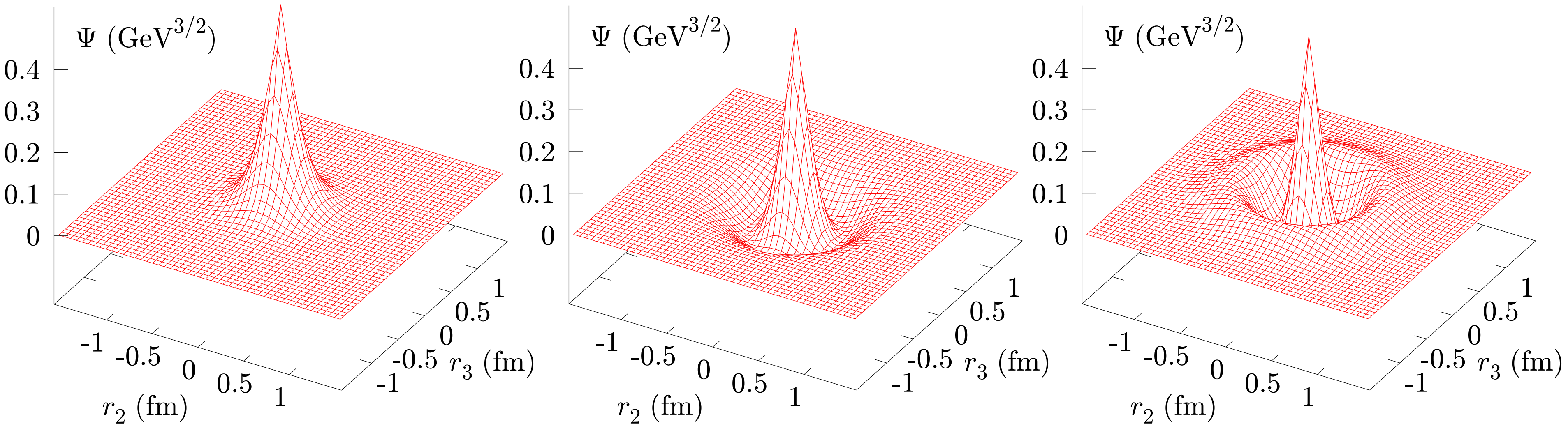


Good overlap with bottomonium states but

$C_{ij}(t) = \langle O_i(t) O_j^\dagger(0)\rangle \neq 0$ for $i \neq j$

$O_i \to \tilde{O}_\alpha = \Omega_{\alpha j} O_j$ such that
$\langle \tilde{O}_\alpha(t)\tilde{O}_\beta^\dagger(0)\rangle \propto \delta_{\alpha,\beta}$
$\Omega_{\alpha j}$ can be obtained as
$G_{ij}(t)\Omega_{\alpha j} = \lambda_\alpha(t,t_0) G_{ij}(t_0)\Omega_{\alpha j}$.

# Back-up: Lattice results on bottomonium spectrum

$\Delta M = M - \overline{M}(1S), \quad \overline{M}(1S) = (M_{\eta_b(1S)} + 3M_{\Upsilon(1S)})/4$

| state | $\Delta M$ [MeV] | $\Delta M(PDG)$ [MeV] |
|---|---|---|
| $\Upsilon(3S)$ | 906.0(25.0)(5.2) | 910.3(0.7) |
| $h_b(2P)$ | 804.4(35.8)(4.7) | 814.9(1.3) |
| $\chi_{b2}(2P)$ | 809.2(36.2)(4.7) | 823.8(0.9) |
| $\chi_{b1}(2P)$ | 802.2(34.9)(4.7) | 810.6(0.7) |
| $\chi_{b0}(2P)$ | 786.8(32.7)(4.6) | 787.6(0.8) |
| $\Upsilon(2S)$ | 582.7(9.8)(3.4) | 578.4(0.6) |
| $h_b(1P)$ | 454.5(4.7)(2.6) | 454.4(0.9) |
| $\chi_{b2}(1P)$ | 463.3(4.8)(2.7) | 467.3(0.6) |
| $\chi_{b1}(1P)$ | 448.9(4.6)(2.6) | 447.9(0.6) |
| $\chi_{b0}(1P)$ | 421.3(4.7)(2.4) | 414.5(0.7) |
| hyperfine(3S) | 13.4(6.2)(0.1) | NA |
| hyperfine(2S) | 24.1(1.0)(0.1) | 24.5(4.5) |

Larsen, Meinel, Mukherjee, PP,
PLB 800 (20) 135119

Prediction for $\eta_b(3S)$ !

$1S$ hyperfine splitting, $M_{\Upsilon(1S)} - M_{\eta_b(1S)}$ is not reproduced within this approach because it is very sensitive to short distance physics $\Rightarrow$ need radiative correction in the NRQCD Lagrangian Dowdal et al (HPQCD), PRD 85 (12) 054509; PRD 89 (14) 031502(R)

or relativistic approach Hatton et al, PRD 103 (21) 054512

For charmonium it is better to use relativistic lattice formulation, Burch et al, PRD 81 (2010) 034508

# Back-up: Bottomonium Bethe-Salpeter amplitude at T>0

$\Upsilon(3S)$

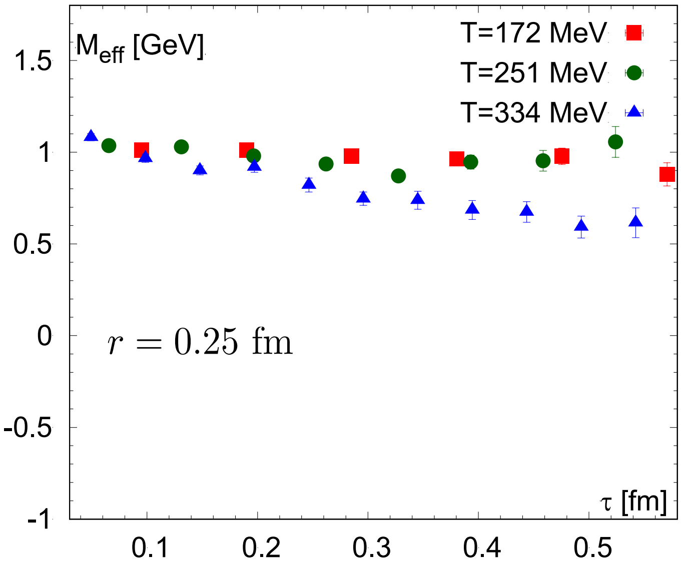


$\Upsilon(3S)$

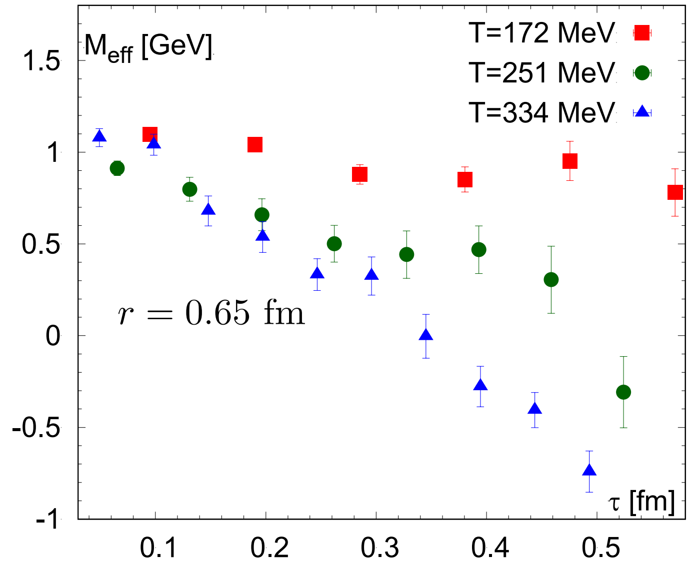


$M_{eff}$ shows similar thermal effects similar to one obtained from optimized correlators;

Thermal effects are larger for larger $r$

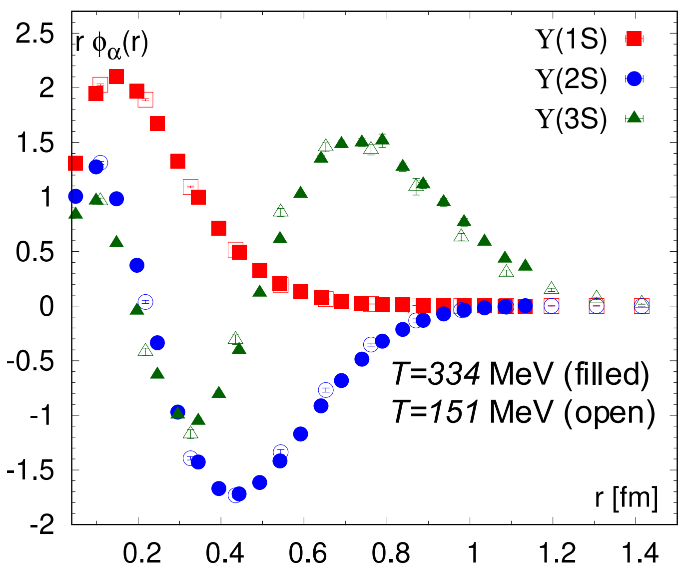


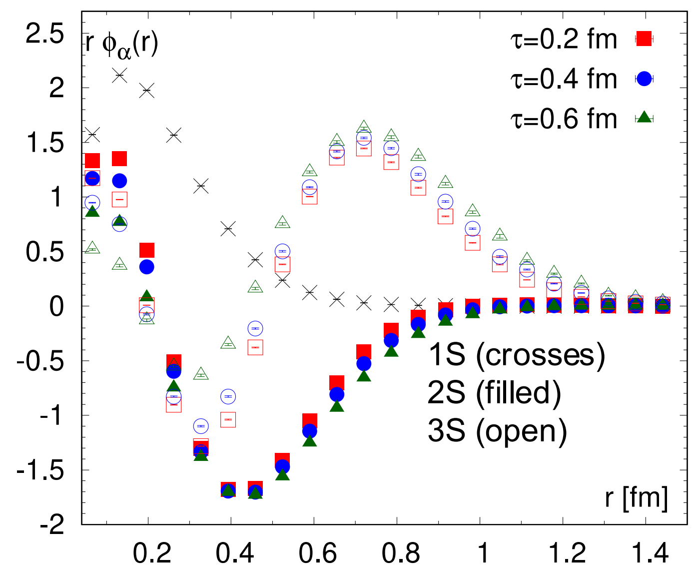


Thermal effects can be seen but $\phi_\alpha$ is similar to the $T = 0$ result at qualitative level

# Back-up:Comparison of different Meson Operators

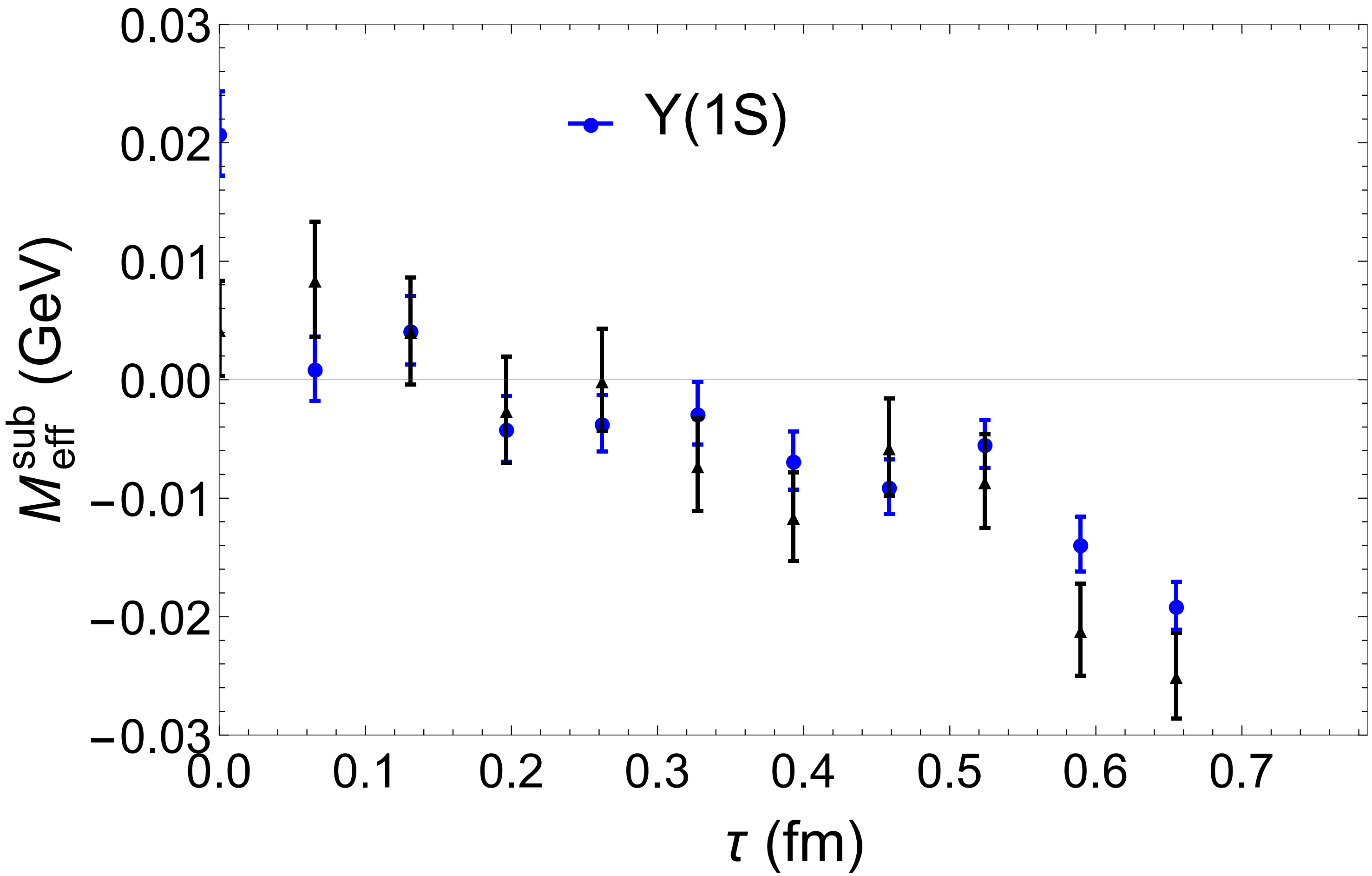


Blue circles: optimized operators

Black triangles: extended operators with Gaussian smearing

T=195 MeV:

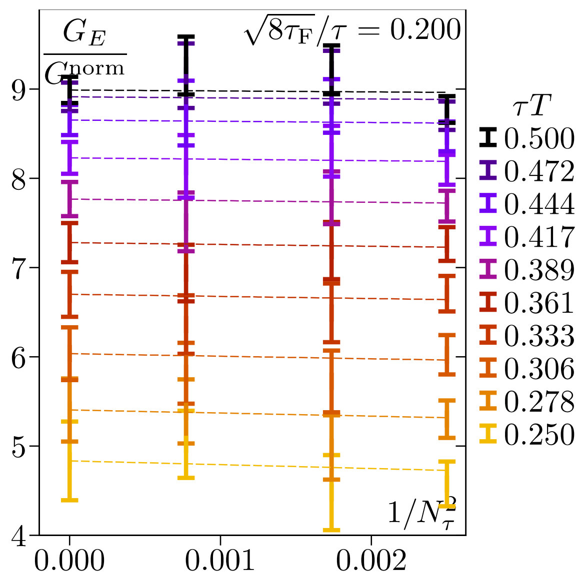

$\frac{G_E}{G^{\mathrm{norm}}}$
$\sqrt{8\tau_F}/\tau = 0.200$
$\tau T$
0.500
0.472
0.444
0.417
0.389
0.361
0.333
0.306
0.278
0.250
$1/N_\tau^2$
0.000
0.001
0.002


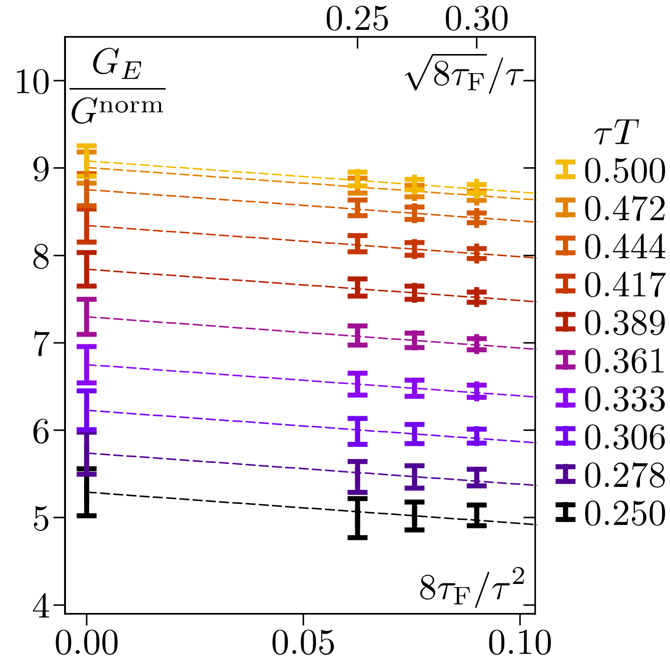

0.25
0.30
$\frac{G_E}{G^{\mathrm{norm}}}$
$\sqrt{8\tau_F}/\tau$
$\tau T$
0.500
0.472
0.444
0.417
0.389
0.361
0.333
0.306
0.278
0.250
$8\tau_F/\tau^2$
0.00
0.05
0.10


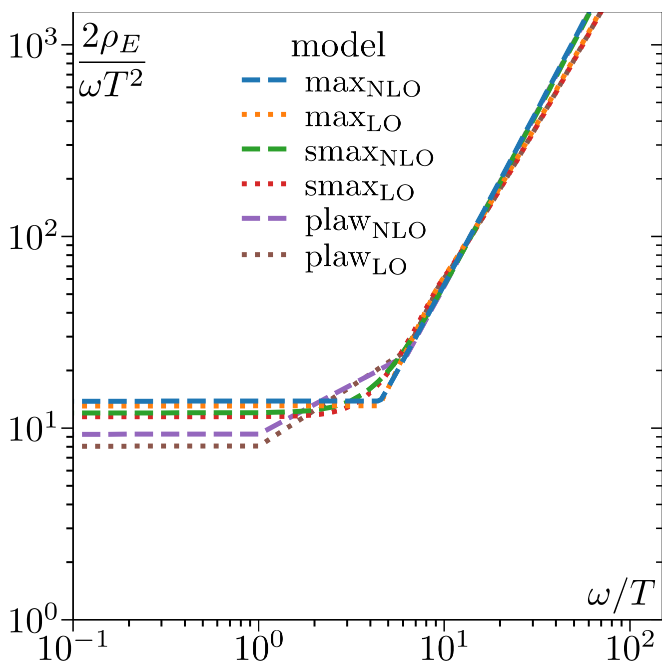

$\frac{2\rho_E}{\omega T^2}$
model
$\mathrm{max_{NLO}}$
$\mathrm{max_{LO}}$
$\mathrm{smax_{NLO}}$
$\mathrm{smax_{LO}}$
$\mathrm{plaw_{NLO}}$
$\mathrm{plaw_{LO}}$
$\omega/T$


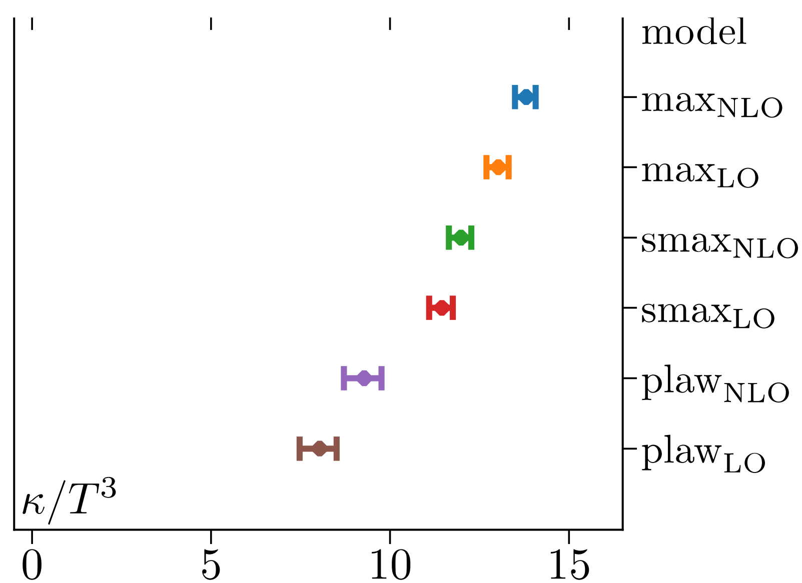

model
$\mathrm{max_{NLO}}$
$\mathrm{max_{LO}}$
$\mathrm{smax_{NLO}}$
$\mathrm{smax_{LO}}$
$\mathrm{plaw_{NLO}}$
$\mathrm{plaw_{LO}}$
$\kappa/T^3$
0
5
10
15

# T=293 MeV:

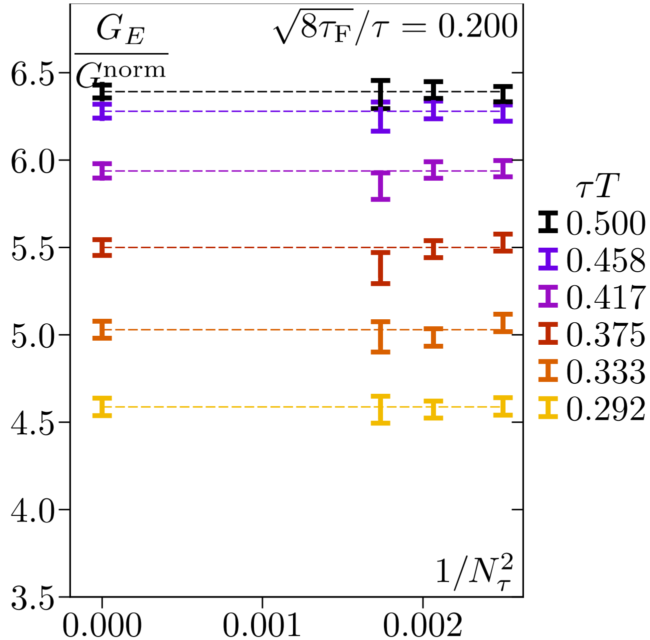

$\frac{G_E}{G^{\mathrm{norm}}}$
$\sqrt{8\tau_{\mathrm{F}}}/\tau = 0.200$
$\tau T$
0.500
0.458
0.417
0.375
0.333
0.292
$1/N_\tau^2$
3.5
4.0
4.5
5.0
5.5
6.0
6.5
0.000
0.001
0.002


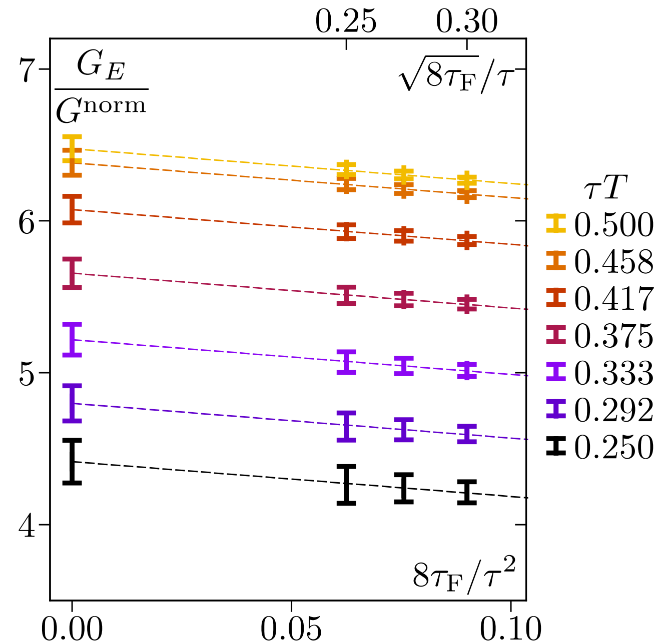

$\frac{G_E}{G^{\mathrm{norm}}}$
$\sqrt{8\tau_{\mathrm{F}}}/\tau$
0.25
0.30
$\tau T$
0.500
0.458
0.417
0.375
0.333
0.292
0.250
$8\tau_{\mathrm{F}}/\tau^2$
4
5
6
7
0.00
0.05
0.10


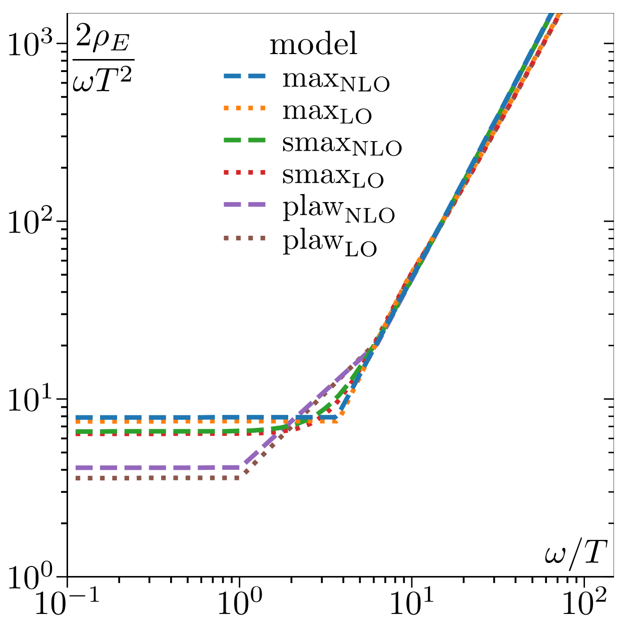

$\frac{2\rho_E}{\omega T^2}$
model
$\mathrm{max_{NLO}}$
$\mathrm{max_{LO}}$
$\mathrm{smax_{NLO}}$
$\mathrm{smax_{LO}}$
$\mathrm{plaw_{NLO}}$
$\mathrm{plaw_{LO}}$
$\omega/T$
$10^0$
$10^1$
$10^2$
$10^3$
$10^{-1}$


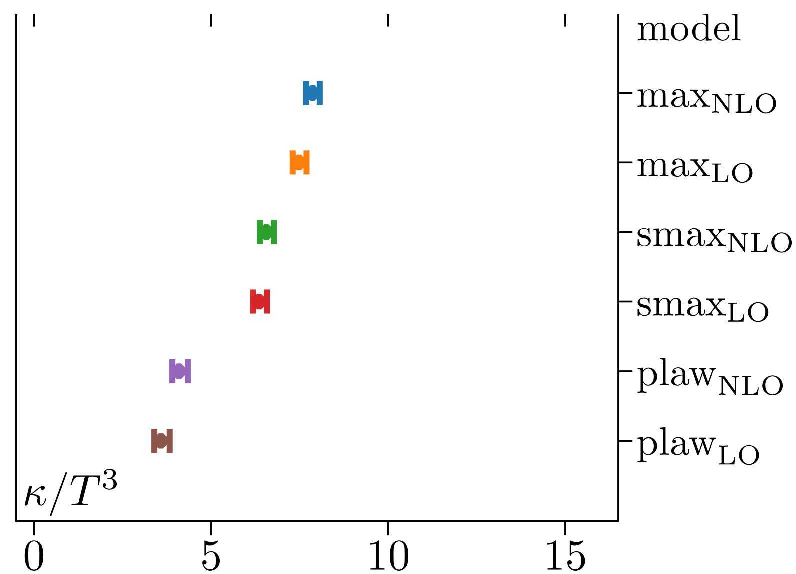

model
$\mathrm{max_{NLO}}$
$\mathrm{max_{LO}}$
$\mathrm{smax_{NLO}}$
$\mathrm{smax_{LO}}$
$\mathrm{plaw_{NLO}}$
$\mathrm{plaw_{LO}}$
$\kappa/T^3$
0
5
10
15